

Figure 8. PAPST-dependent sulfation contributes to mESCs in both undifferentiated and differentiated state. (A) *In vitro* differentiation flowchart of mESCs. EBs that are not treated with RA produce cells from all three germ layers (endoderm, mesoderm and ectoderm) whereas RA-treated EBs produce neurons after further adherent culture. (B) PAPT-dependent sulfation of HS chains regulates the extrinsic signaling (by BMP, FGF and Wnt) that is required for the growth and pluripotency of mESCs, the transduction of extrinsic signals is dependent on the sulfation of HS chains, but not CS chains, and this maintains growth and pluripotency. As shown in this study, autocrine/paracrine FGF signaling contributes to the growth of mESCs. In particular, FGF4 signaling contributes to the differentiation state of the mESCs [23]. (C) PAPT-dependent sulfation of both HS and CS chains regulates the extrinsic signaling (by BMP, FGF and Wnt) that is required for normal differentiation of EBs. During EB differentiation into the three germ layers, the transduction of the extrinsic signals is dependent on the sulfation of both HS and CS chains.

Wnt and BMP signaling inhibit ectodermal differentiation and contribute to mesodermal and definitive endodermal differentiation [20–22,24,25,63]. FGF/ERK and FGF/Akt signaling contribute to mesodermal and definitive endodermal differentiation and primitive ectodermal and visceral endodermal differentiation, respectively [20,61,62]. (D) PAPT-dependent sulfation of HS and CS chains regulates the extrinsic signaling (by BMP, Wnt and FGF) that is required for neuronal differentiation of RA-treated EBs. During RA-treated EB differentiation, the transduction of extrinsic signals is dependent on the sulfation of both HS and CS chains and results in neuronal differentiation. Wnt and BMP signaling inhibit neurogenesis [24,25] and FGF (e.g., bFGF) signaling may contribute to neurogenesis. CS chains regulate Wnt signaling negatively, presumably by sequestering Wnt proteins and preventing them interacting with Wnt receptors. doi:10.1371/journal.pone.0008262.g008

Sulfation of both HS and CS chains contributed to the decision between ectodermal and mesodermal fates by regulating BMP and Wnt signaling (Figure 8C). It is known that signaling by both BMP and Wnt is essential for this decision [21,22,63]. The reduction of BMP and Wnt signaling inhibits mesodermal differentiation and enhances ectodermal differentiation. As shown in Figure 5A and 7A, during EB formation, ectodermal differentiation was promoted in *PAPT-KD* cells and both BMP and Wnt signaling were reduced, which demonstrated that the adoption of an ectodermal fate was enhanced in *PAPT-KD* cells, mainly due to the reduction of these two types of signaling.

Furthermore, sulfation of both HS and CS chains regulated BMP, FGF and Wnt signaling during neural differentiation of EBs after RA treatment. Decreased signaling in *PAPT-KD* cells promoted both the production of neural precursor cells and further neural differentiation (Figure 6, 7A and 8D). Neural specification, which can be achieved by the formation of ESC spheres, has been shown to require signaling by endogenous FGF (e.g. bFGF). FGF signaling that is regulated by the sulfation of both HS and CS chains may also contribute to neurogenesis in RA-treated EBs (Figure 8D). On the other hand, previous reports have demonstrated that signaling by BMP and Wnt inhibits the neurogenesis of mESCs via EB formation [24,25]. As described above, neurogenesis was promoted in *PAPT-KD* cells. Taken together, these results suggest that the reduction of BMP and Wnt signaling mainly affects the promotion of neurogenesis.

As shown in Figure 7B and 8D, HS chains regulate Wnt signaling positively in RA-treated EBs, whereas CS chains regulate the signaling negatively. However, Wnt signaling was reduced overall in RA-treated *PAPT-KD* cells during EB formation (Figure 7A), which indicated that the contribution of HS chains predominated. CS chains have been proposed to function in two distinct ways: they can interact with a ligand either to present it to its receptor (positive function) or to sequester it from its receptor (negative function) [64]. However, the factors that distinguish these two functions have not yet been clarified. It has been demonstrated that the binding of CS chains to ligands, including heparin binding growth-associated molecules, is regulated by the length of the chains and the nature of the sulfated structures [65], which change during development and vary among different tissues and core proteins. With respect to Wnt signaling, CS chains exhibited a negative function in EBs treated with RA but a positive function in untreated EBs, as shown in Figure 7B. These different effects of CS chains on Wnt signaling may depend on the length and sulfated structures of the CS chains, including the core proteins. Furthermore, it has been demonstrated that neural stem/progenitor cells depleted for CS chains are impaired in neuronal differentiation [66], but the underlying mechanisms have not been elucidated. As mentioned above, Wnt signaling contributes to the inhibition of neural differentiation. Thus, we propose that CS

chains promote the differentiation of neural stem/progenitor cells into the neuronal lineage by sequestering Wnt proteins away from their receptors and inhibiting Wnt signaling (Figure 8D).

Johnson et al. [39] have reported recently that HS-null mESCs show no defects in pluripotency, e.g. there is no reduction in *Ocl3/4* expression, but neural differentiation in these cells is disrupted due to defects in FGF4 signaling. Their results differ from ours in certain aspects. 1) A previous report [37] had shown that, in HS-null mESCs, the amount of CS chains is increased, whereas in HS-KD mESCs, this increase is not observed, as had been described previously [17]. In HS-null mESCs, the additional CS chains might contribute to different signaling pathways and compensate for the function of HS chains. 2) Their protocol for neural differentiation was different from ours. They used a Sox1-EGFP reporter cell line in adherent culture: under these culture conditions neural differentiation is induced by autocrine FGF4 signaling [60]. On the other hand, we used EB formation plus RA treatment: under these conditions autocrine signaling by BMP and Wnt inhibits neural differentiation [24,25]. Thus, the different results with respect to neural differentiation could be caused by the use of different culture conditions that induce neural differentiation by different signaling pathways.

The sulfation patterns of HS chains are tissue specific and mutations in enzymes that are involved in HS chain sulfation lead to severe developmental abnormalities [36,38,43]. Thus, control of HS chain structure is essential for the spatiotemporal regulation of cellular differentiation and growth throughout development. However, the patterning of HS chain modification during development has not been well characterized. Recently, it has been demonstrated that the concentration of PAPS influences the patterning of HS chain sulfation in a cooperative manner with NDST [67]. We propose that PAPSTs play important roles in regulating the sulfation levels and patterning of CS chains, as well as HS chains and other sulfated substrates, in a developmental context and contribute to several signaling pathways that are required for normal development.

Materials and Methods

Materials

GDP-[2-³H]mannose (40 Ci/mmol), UDP-[1-³H]glucose (20 Ci/mmol), UDP-*N*-acetyl [6-³H]D-galactosamine (20 Ci/mmol), UDP-*N*-acetyl [6-³H(N)]D-glucosamine (60 Ci/mmol), UDP-[¹⁴C(U)]glucuronic acid (300 mCi/mmol), UDP-[¹⁴C(U)]xylose (264 mCi/mmol), UDP-[6-³H]galactose (20 Ci/mmol), and carrier-free [³⁵S]Na₂SO₄ (100 mCi/ml) were purchased from American Radio-labeled Chemicals Inc. GDP-[2-³H]fucose (17.5 Ci/mmol), CMP-[9-³H]sialic acid (33.6 Ci/mmol), and [³⁵S]PAPS (1.66 Ci/mmol) were purchased from Perkin Elmer Life Sciences Inc. Zymolyase 100T was obtained from Seikagaku Corp. All the other reagents used in this study were of the highest purity grade available commercially.

Cell Culture and Transfection

R1 [68] and E14TG2a [69] mESC lines were maintained on mouse embryonic fibroblasts (MEFs) inactivated with 10 μg/ml mitomycin C (Sigma) in ESC medium (DMEM supplemented with 15% FBS {Hyclone}, 1% penicillin/streptomycin {Gibco}, 0.1 mM 2-mercaptoethanol {Gibco}, and 0.1 mM non-essential amino acids {Gibco}) with 1000 U/ml LIF (Chemicon). We generated siRNA expression plasmids that targeted *PAPST1*, *PAPST2*, *NDST1*, *NDST2*, and *EGFP*, a negative control, by inserting the appropriate dsDNAs between the BamHI and HindIII sites of pSilencer 3.1-H1 (Ambion) or pSUPER.retro.puro (OligoEngine). The siRNA sequences used for RNAi were designed as

described previously [70] using “siDirect”, which is based on accelerated off-target search algorithm [71] and are listed in Table S1. We designed two kinds of constructs, *PAPST1-1* and -2, *PAPST2-1* and -2, *NDST1-1* and -2, and *NDST2-1* and -2, targeting *PAPST1*, *PAPST2*, *NDST1*, and *NDST2*, respectively. We describe mESCs that have been transfected with *EGFP* siRNA expression vectors as “control cells” throughout this paper.

For transient knockdown of *PAPST* or *NDST* mRNA by RNAi, siRNA expression plasmids for *PAPST* or *NDST* were transfected into mESCs as follows. Prior to transfection, the mESCs were harvested, replated at 1×10⁶ cells on gelatin-coated feeder-free 60 mm tissue culture dishes (Iwaki) in ESC medium with LIF, and incubated for 16 h. On day 1, the cells were transfected with an siRNA expression plasmid (2 μg per culture dish) using Lipofectamine 2000 (Invitrogen). On day 2, the cells were harvested and replated at 3×10⁶ cells on gelatin-coated feeder-free 60 mm tissue culture dishes in ESC medium with LIF and 2 μg/ml puromycin (Sigma). In general, puromycin selection of transfected cells was carried out for 24 h. Transfection efficiency was approximately 60%, but only transfected cells survived after puromycin selection. On day 3 (two days after transfection), the transfected cells were harvested and analyzed as described below.

Stable knockdown of *PAPST* mRNA was carried out as follows. To produce retrovirus, the pSUPER.retro.puro constructs were transfected into ecotropic virus-packaging (PLAT-E) cells. Virus-containing supernatants derived from these PLAT-E cultures were mixed with 8 μg/ml polybrene (Sigma) and mESCs were incubated with the virus/polybrene mixtures for 24 h. After infection, the cells were replated with ESC medium containing LIF and 2 μg/ml puromycin and cultured for 5–7 days.

For EB formation, the cells were transferred to Low Cell Binding 60 mm dishes (Nunc) and cultured in ESC medium without LIF. For neuronal differentiation, 1 μM RA (Sigma) was added on day 4 and day 6 after EB formation [72]. On day 8, 200 EBs were plated onto PDL/laminin-coated 60 mm dishes (Becton Dickinson) in DMEM-F12 containing N2 supplement (Gibco). The medium was replaced every other day and the cells were incubated for 6 days.

Metabolic Labeling

To measure total sulfate incorporation into cellular proteins, 3×10⁶ mESCs were replated 2 days after transfection on gelatin-coated 60 mm dishes and incubated in sulfate-free ESC medium with LIF, puromycin and 100 μCi/ml [³⁵S]Na₂SO₄. After labeling for 24 h, the cells were washed with Phosphate Buffered Saline (PBS) and lysed with lysis buffer (50 mM Tris-HCl pH 7.4, 150 mM NaCl, 1% Triton X-100, protease inhibitors). Fifty micrograms of protein were precipitated with 10% trichloroacetic acid and washed with 5% trichloroacetic acid, followed by cold acetone. The precipitate was dried, dissolved in 0.5 N NaOH and the amount of radioactivity present was quantitated using a scintillation counter.

To measure sulfate incorporation into cell surface HS and CS chains, after labeling, the cells were washed twice with PBS and then treated with 1 mg/ml trypsin (WAKO) for 10 min at 37°C. The trypsin was neutralized with 2 mg/ml trypsin inhibitor (Roche). After centrifugation, the supernatants were treated with 0.5 M NaOH at 4°C overnight and neutralized with 1 M acetic acid. The cell pellets were used for normalization as described below. The labeled O-linked glycans were desalted in a PD-10 column (GE Healthcare) and GAG chains were isolated by anion exchange chromatography on HiTrap DEAE FF (GE Healthcare) using sodium phosphate buffer (pH 6.0) containing 1.0 M NaCl as the eluent. After desalting, GAG chains were incubated in the

presence of 5 mU heparitinase I and II (Seikagaku Corp.) or 100 mU/ml ChABC (Seikagaku Corp.) at 37°C overnight. The lyase products of HS or CS were recovered with Microcon YM-3 ultrafiltration devices (*Mfr* 3,000 cut-off; Millipore). The amount of radioactivity present was quantified using a scintillation counter. For normalization of the radioactivity with total amount of protein, the cells pellets obtained as above were lysed with lysis buffer and then the protein was quantified.

To measure molecular size of HS and CS chains, preparation and measurement of ³⁵S-labeled HS and CS chains were performed as described previously [17].

Isolation of Mouse PAPS Transporter cDNA and Construction of Expression Plasmids

The mouse *PAPST1* and *PAPST2* genes were identified and cloned using the same procedures as described previously [31]. To obtain the cDNA of NM_028662 and NM_134060, mouse genes that were identified in this study, and to create recombination sites for the GATEWAYTM cloning system (Invitrogen), we used two steps of *attB* adaptor PCR and prepared *attB*-flanked PCR products. The first gene-specific amplification was performed using Platinum[®] Pfx DNA polymerase (Invitrogen), a cDNA from mESCs and the following primers: *PAPST1*, forward primer with *attB1*, 5'-AAAAAGCAGGCTTCGCCGCCACCATGGACGCCAGATGTGG-3' and a reverse primer with *attB2*, 5'-AGAAAGCTGGGTTACCTTCTGTACTGGGG-3'; *PAPST2*, forward primer with *attB1*, 5'-AAAAAGCAGGCTTCGCCGCCACCATGGACCTCAAGTTCAACAAC-3' and a reverse primer with *attB2*, 5'-AGAAAGCTGGGTTACAGTCTGTGCCA-CGTC-3'. The insertion of a complete *attB* adaptor and cloning into the pDONRTM201 vector were performed in accordance with the manufacturer's protocol to create an entry clone for use during the subsequent subcloning steps. The entry clone was subcloned into a yeast expression vector, YEp352GAP-II [73], by using the GATEWAYTM cloning system in accordance with the manufacturer's protocol. A 3 x influenza HA epitope tag was inserted into the expression vectors at the position corresponding to the C terminus of the expressing protein.

Subcellular Fractionation of Yeast and Transport Assay

Yeast (*Saccharomyces cerevisiae*) strain W303-1a (*MATa*, *ade2-1*, *ura3-1*, *his3-11,15*, *trp1-1*, *leu2-3,112*, and *can1-100*) was transformed by the lithium acetate procedure using YEp352GAP-II inserted with HA-tagged *PAPST1* or *PAPST2*. These transformed yeast cells were grown at 25°C in a synthetic defined medium, which did not contain uracil, for selecting transformants. Subcellular fractionation and nucleotide sugar transport assays were performed as described previously [31]. The cells were harvested, washed with ice-cold 10 mM Na₃N, and converted into spheroplasts by incubation at 37°C for 20 min in spheroplast buffer (1.4 M sorbitol, 50 mM potassium phosphate pH 7.5, 10 mM Na₃N, 40 mM 2-mercaptoethanol, and 1 mg of Zymolyase 100T/g of cells). The spheroplasts were pelleted using a refrigerated centrifuge and washed twice with 1.0 M ice-cold sorbitol to remove traces of zymolyase. The cells were suspended in ice-cold lysis buffer (0.8 M sorbitol in 10 mM triethanolamine pH 7.2, 5 μg/ml of pepstatin A, and 1 mM phenylmethylsulfonyl fluoride) and subsequently homogenized using a Dounce homogenizer. The lysate was centrifuged at 1,000×g for 10 min to remove the unlysed cells and cell wall debris. The supernatant was then centrifuged at 10,000×g for 15 min at 4°C, which yielded a pellet of P10 membrane fraction. The supernatant was further centrifuged at 100,000×g to yield a pellet of P100 Golgi-rich membrane fraction. Each Golgi-rich membrane fraction (100 μg

of protein) was then incubated in 50 μl of reaction buffer (20 mM Tris-HCl pH 7.5, 0.25 M sucrose, 5.0 mM MgCl₂, 1.0 mM MnCl₂, and 10 mM 2-mercaptoethanol) that contained 1 μM radiolabeled substrate at 32°C for 5 min. After incubation, the radioactivity incorporated in the microsomes was trapped using a 0.45-μm nitrocellulose filter (Advantec MFS) and measured using liquid scintillation. The amount of incorporated radioactivity was calculated as the difference from the background value obtained from the same assay for 0 min for each sample.

Measurement of PAPS Transport in mESC

Two days after transfection, cells were harvested and subcellular fractionation and measurement of PAPS transport was performed like as described above. Each Golgi-rich membrane fraction (50 μg of protein) was incubated in 100 μl of reaction buffer that contained 1 μM [³⁵S] PAPS.

FACS Analysis

FACS analysis was performed 3 days after transfection or 8 days after EB formation. Cells were harvested and the cell suspension was incubated with primary antibodies diluted in FACS buffer (0.5% bovine serum albumin (BSA) and 0.1% sodium azide in PBS). After washing, the cell suspension was incubated with FITC-conjugated secondary antibody (Sigma) diluted in FACS buffer. Cell sorting and analysis were performed using a FACSaria Cell Sorter (Becton Dickinson). We used the following as primary antibodies: mouse IgM isotype control (Chemicon), the anti-3'-sulfo-Le^a antibody 91.9H [74], an anti-HNK-1 carbohydrate antibody (Becton Dickinson), the anti-HS antibody 10E4 (Seikagaku Corp.), the anti-HS antibody HepSS-1 (Seikagaku Corp.), the anti-CS antibody 2H6 (Seikagaku Corp.), the anti-SM3 antibody 49-D6 (Seikagaku Corp.) and the anti-SM4 antibody O4 (Chemicon).

Detection of βIII-Tubulin positive cells was performed as follows. Six days after neuronal differentiation, cells were harvested, washed and stained with Propidium Iodide (PI) (Becton Dickinson) to allow the elimination of dead cells by gating. After washing, the cells were fixed with 2% paraformaldehyde and permeabilized with 0.5% saponin. Staining with the primary antibody (anti-βIII-Tubulin antibody; Chemicon) and secondary antibody (FITC-conjugated anti-mouse IgG; Chemicon) was performed in PBS containing 0.1% saponin.

Measurement of Proliferation

Two days after transfection, cells were harvested and replated in triplicate at 0.8×10⁴ cells per well in 96-well 0.2% gelatin-coated plates in ESC medium with LIF. Cell counting kit-8 (Dojindo) was added after 48 h and incubated further for 2 h. The soluble formazan product was measured at 450 nm.

To examine the involvement of autocrine/paracrine FGF signaling in mESC proliferation, we treated mESCs with 10 μM SU5402 (Calbiochem) during culture.

Measurement of Self-Renewal

Two days after transfection, cells were harvested and replated at 1×10⁴ cells per gelatin-coated 60 mm tissue culture dish in ESC medium with LIF. For detection of undifferentiated cells, cells were fixed and stained with BCIP-NBT (Nacalai Tesque) 5 days after replating. Alkaline phosphatase (AP) positive colonies were counted by microscopic examination. Colonies of tightly packed and flattened AP positive cells were counted as undifferentiated, and colonies of mixtures of unstained and stained cells and entirely unstained cells with flattened irregular morphology were considered differentiated.

Analysis of Proteins by Immunoblotting

Three days after transfection, the mESC culture solution was replaced with serum-free ESC medium without LIF for 4 h and the cells were stimulated for 20 min with 1000 U/ml LIF, 10 ng/ml BMP4 (R&D Systems) or 100 ng/ml Wnt3a (R&D Systems), or for 5 min with 40 ng/ml bFGF (Upstate Biotechnology) or 10 ng/ml FGF4 (R&D Systems). To deplete HS or CS chains, mESCs were incubated in the presence of 5 mU heparitinase I and II or 100 mU/ml ChABC for 2 h before stimulation with extrinsic factors. We confirmed the reduction of HS or CS structure by FACS analysis (Figure S8). Cells were lysed with lysis buffer (50 mM Tris-HCl pH 7.4, 150 mM NaCl, 1% Triton X-100, 1 mM Na_3VO_4 , 10 mM NaF, protease inhibitors). Isolation of nuclear extracts was performed as described previously [17]. To deplete HS or CS chains during EB formation, EBs were incubated in the presence of 5 mU heparitinase I and II or 100 mU/ml ChABC, respectively, for 4 days. We confirmed the reduction of HS or CS structure by FACS analysis (Data not shown). For analysis of HA-tagged PAPST1 or PAPST2, protein from each sample was added to 3 x SDS sample buffer (New England Biolabs Inc.) and subsequently incubated at 4°C for 12 h.

Samples containing 5 µg of cell lysate or nuclear extract were separated by 10% SDS-PAGE and transferred onto PVDF membranes (Millipore). After blocking, the membranes were incubated with antibodies against STAT3 (Becton Dickinson), phosphorylated STAT3 (Tyr705; Becton Dickinson), ERK1/2 (Cell Signaling Technology), phosphorylated ERK1/2 (Thr183 and Thr185; Sigma), phosphorylated Smad1 (Ser463 and Ser465; Cell Signaling Technology), β -actin (Sigma), β -catenin (Cell Signaling Technology), Lamin B₁ (Zymed), β III-Tubulin or HA (Roche). The membranes were then incubated with the appropriate peroxidase-conjugated secondary antibodies (Cell Signaling Technology), washed and developed with ECL Plus reagents (GE Healthcare).

Measurement of Luciferase Reporter Activity

Transactivation of β -catenin on T-cell-specific factor (Tcf) was determined with a luciferase reporter assay. siRNA expression plasmid (2 µg) was cotransfected with reporter plasmid such as, TOPFLASH (2 µg, containing three Tcf binding sites, Upstate Biotechnology) or FOPFLASH (2 µg, containing inactive Tcf binding sites, Upstate Biotechnology) and pCH110 (0.2 µg, containing β -galactosidase, GE Healthcare) as control of transfection efficiency using Lipofectamine 2000 as described above. Cell lysates were prepared 3 days after transfection and luciferase activity was measured with Dual-Light® System (Applied Biosystems). To deplete CS chains, cells were incubated in the presence of 100 mU/ml ChABC during cell culture. We confirmed the reduction of CS structure by FACS analysis (Figure S8). Luminescence was measured with a Lumat LB9501 luminometer (Berthold). Luciferase activity was normalized for transfection efficiency by β -galactosidase activity. Relative luciferase activity is defined as the ratio of luciferase activity of TOPFLASH to that of FOPFLASH.

Immunostaining

Six days after replating of EBs on PLL/laminin-coated glass chamber slides (Iwaki) to induce neuronal differentiation, cells were fixed with 4% paraformaldehyde and permeabilized with 0.1% saponin. After washing and subsequent blocking, cells were stained with an anti- β III-Tubulin antibody. After washing, cells were stained with an FITC-conjugated secondary antibody and counterstained with PI. Immunofluorescence images were obtained

using an LSM5Pascal confocal laser scanning microscope (Carl Zeiss).

SPR Analysis

Sugar Chips immobilized with heparin (Nacalai Tesque) or CS-E (Seikagaku Corp.) were purchased from SUDx-Biotec (Kagoshima, Japan) prepared as previously described [17] and were set on a prism with refraction oil ($n_D = 1.518$, Cargill Laboratories Inc.) in an SPR apparatus (SPR670M, Moritex, Yokohama, Japan). The SPR measurements were performed at room temperature in accordance with the manufacturer's instructions and using Tris buffered saline (20 mM Tris-HCl, 150 mM NaCl, pH 7.4) containing 0.05% Tween-20 and 0.1% BSA as the running buffer at a flow rate of 15 µl/min. The kinetic binding parameters were calculated using the software of the manufacturer.

RT-PCR and Real Time PCR

Total RNA was isolated from cells by TRIZOL Reagent (Invitrogen) and subsequently reverse transcribed using an oligo-dT primer (Invitrogen) and a SuperscriptII first strand synthesis kit (Invitrogen). Real time PCR was performed using an ABI PRISM® 7700 sequence detection system (Applied Biosystems). The relative amounts of each mRNA were normalized by β -actin mRNA in the same cDNA. Primer sets for RT-PCR and primer sets and probes for real time PCR are listed in Tables S2, S3 and S4, respectively.

Supporting Information

Figure S1 PAPS transport activity. The results are shown after normalization against the values obtained with control cells (value = 1). The values shown are the means \pm SD of three independent experiments and significant values are indicated; * $P < 0.05$, in comparison to the control.

Found at: doi:10.1371/journal.pone.0008262.s001 (0.14 MB TIF)

Figure S2 (A) Photomicrographs of cells 4 days after transfection. Representative photographs of control and PAPST-KD cells from two independent experiments are shown. Scale bar, 50 µm. (B) Real time PCR analysis of germ layer markers (*Gata6*, primitive endoderm; *LamininB1*, parietal endoderm; *Bmp2*, visceral endoderm; *Cdx2*, trophoblast; *Fgf-5*, primitive ectoderm; *Isl1*, neuroectoderm; *Brachyury*, mesoderm) in the cells 4 days after transfection. The results are shown after normalization against the values obtained with control cells (value = 1). The values shown are the means \pm SD from two independent experiments. (open bars, control cells; solid bars, from left, PAPST1-KD, PAPST2-KD, PAPST1+2-KD, and NDST1+2-KD cells, respectively).

Found at: doi:10.1371/journal.pone.0008262.s002 (2.40 MB TIF)

Figure S3 (A) Self-renewal assay. The ratio of alkaline phosphatase positive colonies is shown after normalization against the ratio obtained with non-treated cells (value = 1). The values shown are the means \pm SD from three independent. (B) Proliferation assay. The ratio of proliferation 48 h after culture is shown after normalization against the values obtained with non-treated cells (value = 1). The values shown are the means \pm SD from three independent experiments. (C) Luciferase reporter assay. Relative luciferase activities (TOPFLASH/FOPFLASH) are shown as means \pm SD from three independent experiments after normalization against the values obtained with non-treated cells (value = 1). In (A) – (C), cells were incubated in the presence of 100 mU/ml ChABC during cell culture. We confirmed the reduction of CS structure by FACS analysis (Figure S8).

Found at: doi:10.1371/journal.pone.0008262.s003 (0.64 MB TIF)

Figure S4 (A) RT-PCR analysis of the expression of several *FGFs* and *FGFRs* in mESCs and MEFs. (B) Proliferation assay. The ratio of proliferation 48 h after culture is shown after normalization against the values obtained with DMSO-treated cells (value = 1). The values shown are the means \pm SD from three independent experiments and significant values are indicated; * $P < 0.01$, in comparison to DMSO-treated cells.

Found at: doi:10.1371/journal.pone.0008262.s004 (1.98 MB TIF)

Figure S5 Western blot analysis of cells 3 days after transfection. Representative immunoblots are shown. The histograms show mean densitometric readings \pm SD of β -catenin/Lamin B1 after normalization against the values obtained with control cells (value = 1). Values were obtained from duplicate measurements of two independent experiments and significant values are indicated; * $P < 0.01$, in comparison to the control.

Found at: doi:10.1371/journal.pone.0008262.s005 (0.52 MB TIF)

Figure S6 Western blot analysis 6 days after replating of EBs. Representative immunoblots are shown. The histograms show mean densitometric readings \pm SD of β III-Tubulin/ β -actin after normalization against the values obtained with control cells not treated with RA (value = 1). Values were obtained from duplicate measurements of two independent experiments and significant values are indicated; * $P < 0.03$, in comparison to the control.

Found at: doi:10.1371/journal.pone.0008262.s006 (0.84 MB TIF)

Figure S7 (A) FACS analysis of RA-treated and non-treated EBs using an anti-CS antibody or anti-HS (HepSS-1) antibody. Black line represents IgM isotype control. Three independent experiments were performed and representative results are shown. (B) FACS analysis of RA-treated EBs using an anti-HNK-1 antibody. Black line represents IgM isotype control. Three independent experiments were performed and representative results are shown. Found at: doi:10.1371/journal.pone.0008262.s007 (0.61 MB TIF)

Figure S8 (A) FACS analysis of heparitinase-treated or ChABC-treated mESCs using an anti-HS (10E4) antibody or anti-CS antibody. Black line represents IgM isotype control. Three independent experiments were performed and representative results are shown.

Found at: doi:10.1371/journal.pone.0008262.s008 (0.35 MB TIF)

Table S1 The single-stranded DNA oligonucleotide sequence Found at: doi:10.1371/journal.pone.0008262.s009 (0.05 MB DOC)

Table S2 List of gene specific primers for RT-PCR Found at: doi:10.1371/journal.pone.0008262.s010 (0.05 MB DOC)

Table S3 List of gene specific primers for real time PCR Found at: doi:10.1371/journal.pone.0008262.s011 (0.06 MB DOC)

Table S4 List of gene specific probes for real time PCR Found at: doi:10.1371/journal.pone.0008262.s012 (0.05 MB DOC)

Acknowledgments

We thank Prof. Tatsuro Irimura, Prof. Toshio Kitamura and Prof. Kumiko Ui-Tei for gifting experimental materials. We thank Prof. Kazunari Hanaoka and Michiko Hayasaka for blastocyst injection. We thank Akio Saito, Takao Kondo, and Maiko Tokito for syntheses of sugar chains, as well as Yuko Kishimoto and Tomoaki Nishimura (SUDx-Biotec Corporation) for the SPR imaging.

Author Contributions

Conceived and designed the experiments: NS SN. Performed the experiments: NS TH TI MW KH AKT. Analyzed the data: NS TI HT YS. Contributed reagents/materials/analysis tools: YS. Wrote the paper: NS SN.

References

- Evans MJ, Kaufman MH (1981) Establishment in culture of pluripotential cells from mouse embryos. *Nature* 292: 154–156.
- Martin GR (1981) Isolation of a pluripotent cell line from early mouse embryos cultured in medium conditioned by teratocarcinoma stem cells. *Proc Natl Acad Sci U S A* 78: 7634–7638.
- Keller G (2005) Embryonic stem cell differentiation: emergence of a new era in biology and medicine. *Genes Dev* 19: 1129–1155.
- Chambers I, Smith A (2004) Self-renewal of teratocarcinoma and embryonic stem cells. *Oncogene* 23: 7150–7160.
- Ivanova N, Dobrin R, Lu R, Koteenko I, Levorse J, et al. (2006) Dissecting self-renewal in stem cells with RNA interference. *Nature* 442: 533–538.
- Boiani M, Scholer HR (2005) Regulatory networks in embryo-derived pluripotent stem cells. *Nat Rev Mol Cell Biol* 6: 872–884.
- Smith AG, Heath JK, Donaldson DD, Wong GG, Moreau J, et al. (1988) Inhibition of pluripotential embryonic stem cell differentiation by purified polypeptides. *Nature* 336: 688–690.
- Williams RL, Hilton DJ, Pease S, Willson TA, Stewart CL, et al. (1988) Myeloid leukaemia inhibitory factor maintains the developmental potential of embryonic stem cells. *Nature* 336: 684–687.
- Boeuf H, Hauss C, Gracve FD, Baran N, Kedinger C (1997) Leukemia inhibitory factor-dependent transcriptional activation in embryonic stem cells. *J Cell Biol* 138: 1207–1217.
- Matsuda T, Nakamura T, Nakao K, Arai T, Katsuki M, et al. (1999) STAT3 activation is sufficient to maintain an undifferentiated state of mouse embryonic stem cells. *EMBO J* 18: 4261–4269.
- Niva H, Burdon T, Chambers I, Smith A (1998) Self-renewal of pluripotent embryonic stem cells is mediated via activation of STAT3. *Genes Dev* 12: 2048–2060.
- Raz R, Lee CK, Cannizzaro LA, d'Eustachio P, Levy DE (1999) Essential role of STAT3 for embryonic stem cell pluripotency. *Proc Natl Acad Sci U S A* 96: 2846–2851.
- Cartwright P, McLean C, Sheppard A, Rivett D, Jones K, et al. (2005) LIF/STAT3 controls ES cell self-renewal and pluripotency by a Myc-dependent mechanism. *Development* 132: 885–896.
- Ying QL, Nichols J, Chambers I, Smith A (2003) BMP induction of Id proteins suppresses differentiation and sustains embryonic stem cell self-renewal in collaboration with STAT3. *Cell* 115: 281–292.
- Qi X, Li TG, Hao J, Hu J, Wang J, et al. (2004) BMP4 supports self-renewal of embryonic stem cells by inhibiting mitogen-activated protein kinase pathways. *Proc Natl Acad Sci U S A* 101: 6027–6032.
- Sato N, Meijer L, Skaltsounis L, Greengard P, Brivanlou AH (2004) Maintenance of pluripotency in human and mouse embryonic stem cells through activation of Wnt signaling by a pharmacological GSK-3-specific inhibitor. *Nat Med* 10: 55–63.
- Sasaki N, Okishio K, Ui-Tei K, Saigo K, Kinoshita-Toyoda A, et al. (2008) Heparan sulfate regulates self-renewal and pluripotency of embryonic stem cells. *J Biol Chem* 283: 3594–3606.
- Miyabayashi T, Teo JL, Yamamoto M, McMillan M, Nguyen C, et al. (2007) Wnt/beta-catenin/CBP signaling maintains long-term murine embryonic stem cell pluripotency. *Proc Natl Acad Sci U S A* 104: 5668–5673.
- Hao J, Li TG, Qi X, Zhao DF, Zhao GQ (2006) WNT/beta-catenin pathway up-regulates Stat3 and converges on LIF to prevent differentiation of mouse embryonic stem cells. *Dev Biol* 290: 81–91.
- Loebel DA, Watson CM, De Young RA, Tam PP (2003) Lineage choice and differentiation in mouse embryos and embryonic stem cells. *Dev Biol* 264: 1–14.
- Finley MF, Devata S, Huetner JE (1999) BMP-4 inhibits neural differentiation of murine embryonic stem cells. *J Neurobiol* 40: 271–287.
- Gratsch TE, O'Shea KS (2002) Noggin and chordin have distinct activities in promoting lineage commitment of mouse embryonic stem (ES) cells. *Dev Biol* 245: 83–94.
- Kunath T, Saba-El-Leil MK, Almousailleakh M, Wray J, Meloche S, et al. (2007) FGF stimulation of the Erk1/2 signalling cascade triggers transition of pluripotent embryonic stem cells from self-renewal to lineage commitment. *Development* 134: 2895–2902.
- Haegele L, Ingold B, Naumann H, Tabatabai G, Ledermann B, et al. (2003) Wnt signalling inhibits neural differentiation of embryonic stem cells by controlling bone morphogenetic protein expression. *Mol Cell Neurosci* 24: 696–708.
- Aubert J, Dunstan H, Chambers I, Smith A (2002) Functional gene screening in embryonic stem cells implicates Wnt antagonism in neural differentiation. *Nat Biotechnol* 20: 1240–1245.
- Schwartz NB, Lyle S, Ozeran JD, Li H, Deyrup A, et al. (1998) Sulfate activation and transport in mammals: system components and mechanisms. *Chem Biol Interact* 109: 143–151.

27. Li H, Deyrup A, Mensch JR Jr, Domowicz M, Konstantinidis AK, et al. (1995) The isolation and characterization of cDNA encoding the mouse bifunctional ATP sulfurylase-adenosine 5'-phosphosulfate kinase. *J Biol Chem* 270: 29453–29459.
28. Besset S, Vincourt JB, Amalric F, Girard JP (2000) Nuclear localization of PAPS synthetase 1: a sulfate activation pathway in the nucleus of eukaryotic cells. *FASEB J* 14: 345–354.
29. Kamiyama S, Suda T, Ueda R, Suzuki M, Okubo R, et al. (2003) Molecular cloning and identification of 3'-phosphoadenosine 5'-phosphosulfate transporter. *J Biol Chem* 278: 25958–25963.
30. Luders F, Segawa H, Stein D, Selva EM, Perrimon N, et al. (2003) *slalom* encodes an adenosine 3'-phosphate 5'-phosphosulfate transporter essential for development in *Drosophila*. *EMBO J* 22: 3635–3644.
31. Kamiyama S, Sasaki N, Goda E, Ui-Tei K, Saigo K, et al. (2006) Molecular cloning and characterization of a novel 3'-phosphoadenosine 5'-phosphosulfate transporter, PAPST2. *J Biol Chem* 281: 10945–10953.
32. Goda E, Kamiyama S, Uno T, Yoshida H, Ueyama M, et al. (2006) Identification and characterization of a novel *Drosophila* 3'-phosphoadenosine 5'-phosphosulfate transporter. *J Biol Chem* 281: 28508–28517.
33. Lin X (2004) Functions of heparan sulfate proteoglycans in cell signaling during development. *Development* 131: 6009–6021.
34. Aurelic C, Malgorzata W, Sophia vdH, Melissa AR, Scott BS, et al. (2008) Regulation of zebrafish skeletogenesis by *ext2/dackel* and *papst1/pinscher*. *PLoS Genetics* 7: e1000136.
35. Garcia-Garcia MJ, Anderson KV (2003) Essential role of glycosaminoglycans in Fgf signaling during mouse gastrulation. *Cell* 114: 727–737.
36. Li JP, Gong F, Hagner-McWhirter A, Forsberg E, Abrink M, et al. (2003) Targeted disruption of a murine *glucuronyl C5-epimerase* gene results in heparan sulfate lacking L-iduronic acid and in neonatal lethality. *J Biol Chem* 278: 28363–28366.
37. Lin X, Wei G, Shi Z, Dryer L, Esko JD, et al. (2000) Disruption of gastrulation and heparan sulfate biosynthesis in *EXT1*-deficient mice. *Dev Biol* 224: 299–311.
38. Merry CL, Bullock SL, Swan DC, Backen AC, Lyon M, et al. (2001) The molecular phenotype of heparan sulfate in the *Hs2st*^{-/-} mutant mouse. *J Biol Chem* 276: 35429–35434.
39. Johnson CE, Crawford BE, Stavridis M, Ten Dam G, Wat AL, et al. (2007) Essential alterations of heparan sulfate during the differentiation of embryonic stem cells to Sox1-enhanced green fluorescent protein-expressing neural progenitor cells. *Stem Cells* 25: 1913–1923.
40. Baldwin RJ, ten Dam GB, van Kuppevelt TH, Lacaud G, Gallagher JT, et al. (2008) A developmentally regulated heparan sulfate epitope defines a subpopulation with increased blood potential during mesodermal differentiation. *Stem Cells* 26: 3108–3118.
41. Li F, Shetty AK, Sugahara K (2007) Neurogenic activity of chondroitin/dermatan sulfate hybrid chains of embryonic pig brain and their mimicry from shark liver. Involvement of the pleiotrophin and hepatocyte growth factor signaling pathways. *J Biol Chem* 282: 2956–2966.
42. Maeda N, Fukazawa N, Hata T (2006) The binding of chondroitin sulfate to pleiotrophin/heparin-binding growth-associated molecule is regulated by chain length and oversulfated structures. *J Biol Chem* 281: 4894–4902.
43. Lamanna WC, Baldwin RJ, Padva M, Kalus I, Ten Dam G, et al. (2006) Heparan sulfate 6-O-endosulfatases: discrete *in vivo* activities and functional cooperativity. *Biochem J* 400: 63–73.
44. Dick G, Grondahl F, Prydz K (2008) Overexpression of the 3'-phosphoadenosine 5'-phosphosulfate (PAPS) transporter 1 increases sulfation of chondroitin sulfate in the apical pathway of MDCK II cells. *Glycobiology* 18: 53–65.
45. Holmhorn K, Ledin J, Smeds E, Eriksson I, Kusche-Gullberg M (2004) Heparan sulfate synthesized by mouse embryonic stem cells deficient in NDST1 and NDST2 is 6-O-sulfated but contains no *N*-sulfate groups. *J Biol Chem* 279: 42355–42358.
46. Ogawa K, Saito A, Matsui H, Suzuki H, Ohtsuka S, et al. (2007) Activin-Nodal signaling is involved in propagation of mouse embryonic stem cells. *J Cell Sci* 120: 55–65.
47. Dvorak P, Hampl A, Jirmanova L, Pacholikova J, Kusakabe M (1998) Embryoglycan ectodomains regulate biological activity of FGF-2 to embryonic stem cells. *J Cell Sci* 111: 2945–2952.
48. Sugaya N, Habuchi H, Nagai N, Ashikari-Hada S, Kimata K (2008) 6-O-sulfation of heparan sulfate differentially regulates various fibroblast growth factor-dependent signalings in culture. *J Biol Chem* 283: 10366–10376.
49. Deepa SS, Umehara Y, Higashiyama S, Itoh N, Sugahara K (2002) Specific molecular interactions of oversulfated chondroitin sulfate E with various heparin-binding growth factors. Implications as a physiological binding partner in the brain and other tissues. *J Biol Chem* 277: 43707–43716.
50. Ohkawara B, Iemura S, ten Dijke P, Ueno N (2002) Action range of BMP is defined by its *N*-terminal basic amino acid core. *Current Biol* 12: 205–209.
51. Nadanaka S, Ishida M, Ikegami M, Kitagawa H (2008) Chondroitin 4-O-sulfotransferase-1 modulates Wnt-3a signaling through control of E disaccharide expression of chondroitin sulfate. *J Biol Chem* 283: 27333–27343.
52. Kleene R, Schachner M (2004) Glycans and neural cell interactions. *Nat Rev Neurosci* 5: 195–208.
53. Yanagisawa M, Taga T, Nakamura K, Ariga T, Yu RK (2005) Characterization of glycoconjugate antigens in mouse embryonic neural precursor cells. *J Neurochem* 95: 1311–1320.
54. Yamamoto S, Oka S, Inoue M, Shimuta M, Manabe T, et al. (2002) Mice deficient in nervous system-specific carbohydrate epitope HNK-1 exhibit impaired synaptic plasticity and spatial learning. *J Biol Chem* 277: 27227–27231.
55. Monigatti F, Gasteiger E, Bairoch A, Jung E (2002) The Sulfinator: predicting tyrosine sulfation sites in protein sequences. *Bioinformatics* 18: 769–770.
56. Bernfield M, Gotte M, Park PW, Reizes O, Fitzgerald ML, et al. (1999) Functions of cell surface heparan sulfate proteoglycans. *Annu Rev Biochem* 68: 729–777.
57. Orellana A, Hirschberg CB, Wei Z, Swiedler SJ, Ishihara M (1994) Molecular cloning and expression of a glycosaminoglycan *N*-acetylglucosaminyl *N*-deacetylase/*N*-sulfotransferase from a heparin-producing cell line. 269: 2270–2276.
58. Zhang J, Li L (2005) BMP signaling and stem cell regulation. *Dev Biol* 284: 1–11.
59. Niwa H, Miyazaki J, Smith AG (2000) Quantitative expression of Oct-3/4 defines differentiation, dedifferentiation or self-renewal of ES cells. *Nat Genet* 24: 372–376.
60. Ying QL, Stavridis M, Griffiths D, Li M, Smith A (2003) Conversion of embryonic stem cells into neuroectodermal precursors in adherent monoculture. *Nat Biotechnol* 21: 183–186.
61. Chen Y, Li X, Eswarakumar VP, Seger R, Lonai P (2000) Fibroblast growth factor (FGF) signaling through PI 3-kinase and Akt/PKB is required for embryoid body differentiation. *Oncogene* 19: 3750–3756.
62. Kimmelman D (2006) Mesoderm induction: from caps to chips. *Nat Rev Genet* 7: 360–372.
63. Yoshikawa Y, Fujimori T, McMahon AP, Takada S (1997) Evidence that absence of Wnt-3a signaling promotes neuralization instead of paraxial mesoderm development in the mouse. *Dev Biol* 183: 234–242.
64. Carulli D, Laabs T, Geller HM, Fawcett JW (2005) Chondroitin sulfate proteoglycans in neural development and regeneration. *Curr Opin Neurobiol* 15: 116–120.
65. Maeda N, Fukazawa N, Hata T (2006) The binding of chondroitin sulfate to pleiotrophin/heparin-binding growth-associated molecule is regulated by chain length and oversulfated structures. *J Biol Chem* 281: 4894–4902.
66. Sirko S, von Holst A, Wizemann A, Gotz M, Faissner A (2007) Chondroitin sulfate glycosaminoglycans control proliferation, radial glia cell differentiation and neurogenesis in neural stem/progenitor cells. *Development* 134: 2727–2738.
67. Carlsson P, Presto J, Spillmann D, Lindahl U, Kjellen L (2008) Heparin/heparan sulfate biosynthesis: processive formation of *N*-sulfated domains. *J Biol Chem* 283: 20008–20014.
68. Nagy A, Rossant J, Nagy R, Abramow-Newerly W, Roder JC (1993) Derivation of completely cell culture-derived mice from early-passage embryonic stem cells. *Proc Natl Acad Sci U S A* 90: 8424–8428.
69. Smith AG, Hooper ML (1987) Buffalo rat liver cells produce a diffusible activity which inhibits the differentiation of murine embryonal carcinoma and embryonic stem cells. *Dev Biol* 121: 1–9.
70. Ui-Tei K, Naito Y, Takahashi F, Haraguchi T, Ohki-Hamazaki H, et al. (2004) Guidelines for the selection of highly effective siRNA sequences for mammalian and chick RNA interference. *Nucleic Acids Res* 32: 936–948.
71. Yamada T, Morishita S (2005) Accelerated off-target search algorithm for siRNA. *Bioinformatics* 21: 1316–1324.
72. Bain G, Kitchens D, Yao M, Huettner JE, Gottlieb DI (1995) Embryonic stem cells express neuronal properties *in vitro*. *Dev Biol* 168: 342–357.
73. Nakayama K, Maeda Y, Jigami Y (2003) Interaction of GDP-4-keto-6-deoxymannose-3,5-epimerase-4-reductase with GDP-mannose-4,6-dehydratase stabilizes the enzyme activity for formation of GDP-fucose from GDP-mannose. *Glycobiology* 13: 673–680.
74. Tsuji H, Hong JC, Kim YS, Ikehara Y, Narimatsu H, et al. (1998) Novel carbohydrate specificity of monoclonal antibody 91.9H prepared against human colonic sulfomucin: recognition of sulfo-Lewis(a) structure. *Biochem Biophys Res Commun* 253: 374–381.



Research paper

Interferon- γ release assay: A simple method for detection of varicella-zoster virus-specific cell-mediated immunity

Naruhito Otani^a, Koichi Baba^b, Toshiomi Okuno^{a,*}

^a Hyogo College of Medicine, Department of Microbiology, 1-1, Mukogawa-cho, Nishinomiya, Hyogo 663-8501, Japan

^b Baba Children's Clinic, 43-38, Honmachi, Kadoma, Osaka 571-0046, Japan

ARTICLE INFO

Article history:

Received 11 August 2009

Received in revised form 24 September 2009

Accepted 29 September 2009

Available online 8 October 2009

Keywords:

Varicella-zoster virus
Cell-mediated immunity
Interferon- γ

ABSTRACT

Herpes zoster is closely related to decreased varicella-zoster virus (VZV)-specific cell-mediated immunity. We validated a new assay for measuring VZV-specific immunity. We cultured the whole blood of healthy subjects with live attenuated VZV vaccine. Cultured supernatants were harvested at 24-h intervals and assayed for interferon-gamma (IFN- γ) by an enzyme-linked immunosorbent assay (ELISA). The 48-h culture was suitable for estimating IFN- γ release. IFN- γ production was stable after standing for at least 4 h at room temperature. IFN- γ production was observed in whole blood from subjects with recent VZV infection, but not in blood from subjects naïve to the virus. Thus, the IFN- γ release assay may be useful as a new surrogate assay for measuring VZV-specific immunity.

© 2009 Elsevier B.V. All rights reserved.

1. Introduction

Varicella-zoster virus (VZV) is a member of the alphaherpesvirus subfamily and is the etiological agent of chicken pox. The virus initially infects the upper respiratory tract or the conjunctiva, then disseminates into the bloodstream through peripheral blood mononuclear cells (PBMCs). The virus is transferred from PBMCs to epithelial cells, resulting in infection of the skin and the characteristic rash of varicella (Arvin et al., 1996). VZV is a neurotropic virus and establishes itself in a dormant form in sensory nerve ganglia. Its reactivation results in herpes zoster (HZ), a localized skin rash following the distribution of the nerves arising from the affected ganglion. The most frequent complication following HZ is chronic and often debilitating pain called postherpetic neuralgia (PHN), which can

last for months after the disappearance of a rash. HZ and PHN can have a substantial negative impact on quality of life.

Induction of the innate immune response occurs during acute VZV infection, and cell-mediated and humoral immune responses develop within a few days. VZV-specific antibodies interfere with the initial phases of VZV replication in vivo, as shown by a reduced varicella attack rate (Zaia et al., 1983). Moreover, transplacentally-acquired anti-VZV IgG antibodies are known to protect infants from varicella. In a variety of clinical settings, however, humoral immunity does not appear to correlate with viral reactivation (Arvin and Koropchak, 1980; Webster et al., 1989). Children with agammaglobulinemia have uncomplicated varicella, whereas children with primary cellular immunodeficiency diseases experience progressive varicella infections, which are often fatal (Myers, 1979). A progressive decline in VZV-specific cell-mediated immunity (CMI) that occurs with aging and the absence of an age effect on the levels of VZV antibodies have been demonstrated (Levin et al., 2008). In elderly subjects and immunocompromised patients, the increased risk of HZ is associated with diminished T-cell immunity against VZV (Hata et al., 2002; Levin et al., 2003, 2008; Meyers et al., 1980; Wilson et al., 1992; Zhang et al., 1994). Thus, a substantial amount of evidence indicates that

Abbreviation: CMI, cell-mediated immunity; HZ, herpes zoster; IFN- γ , interferon-gamma; IR, interferon- γ release; PBMCs, peripheral blood mononuclear cells; PHN, postherpetic neuralgia; PHA, phytohemagglutinin; RCF, responder cell frequency; VZV, varicella-zoster virus.

* Corresponding author. Tel.: +81 798 45 6548; fax: +81 798 40 9162.

E-mail address: naruhito@fa2.so-net.ne.jp (T. Okuno).

CMI is more important than humoral immunity in preventing viral infection and reactivation.

VZV is the first human herpes virus for which a vaccine has been developed to prevent primary infection (Takahashi et al., 2008). In addition, it is also considered to be effective in preventing HZ in individuals with suboptimal levels of CMI, such as immunocompromised patients or elderly persons, by boosting CMI (Gershon et al., 1996; Sartori, 2004; Takahashi et al., 2008). Considering the variety of clinical settings in which the VZV vaccine may be administered to prevent HZ, as shown elsewhere (Oxman et al., 2005), the evaluation of VZV-specific CMI is essential for predicting its reactivation.

To date, several methods have been developed to assess VZV-specific immunity, in addition to measuring antibodies to the virus. These methods include the lymphocyte proliferation assay, the responder cell frequency assay, the intracellular cytokine staining assay, the interferon- γ enzyme-linked immunospot assay, the interferon- γ secretion assay, and the skin test. Here, we report a new method, the interferon- γ release (IR) assay, which measures the level of interferon- γ secreted from whole blood after stimulation with the viral particles. This assay is simpler and easier than other *in vitro* assays, and therefore, may be a candidate for use in point-of-care settings.

2. Materials and methods

2.1. Study subjects

Three healthy adults (age, 28–38 years) and 12 children (age, 9 months to 11 years) were enrolled in the study (Table 1). This study was approved by the ethics committee of Hyogo College of Medicine, and blood collection was performed after obtaining informed consent from all subjects or their legal guardians.

2.2. Antibody titration

Anti-VZV antibody titers in the sera were examined by the indirect immunofluorescence test. VZV (Oka vaccine strain)-infected MRC-5 cells were spotted on glass slides, air dried,

and fixed with cold acetone. Serially diluted sera were spotted onto the slides and incubated at 37 °C for 1 h. After the slides were washed with phosphate-buffered saline, fluorescein-conjugated goat antibodies against human IgG or IgM were added to the slides and incubated at 37 °C for 1 h. After the slides were washed, signals were detected by using a fluorescence microscope. The antibody titers were determined as the highest dilution of serum showing a positive signal.

2.3. IR assay

A live varicella vaccine (Oka strain, BIKEN, lot VZ050) with a titer of more than 1×10^4 plaque forming units per dose was used for the IR assay. Next, 100 μ l of heparinized whole blood was plated in flat-bottom microtiter plates and co-cultivated with varying amounts of ultraviolet (UV)-inactivated (2700 J/m²) varicella vaccine diluted twice with Roswell Park Memorial Institute (RPMI) 1640 medium in a final volume of 200 μ l/well. The live vaccine viruses were prepared by reconstitution with distilled water according to the manufacturer's protocol (Biken, Osaka, Japan). Co-cultivations were carried out within 1 h after drawing blood samples from the subjects. One hundred microlitres of culture supernatants was collected 24, 48, or 72 h after cultivation, and IFN- γ concentrations were quantified by using an enzyme-linked immunosorbent assay (ELISA; IFN- γ Assay kit; Biosource International, Camarillo, California) according to the manufacturer's instructions. In order to collect culture supernatants serially, those were harvested from separate parallel cultures prepared for each time points. Either phytohemagglutinin (PHA; final concentration, 2.5 μ g/ml) or medium was added to the blood instead of the varicella vaccine as the positive and negative controls, respectively.

3. Results

3.1. VZV-specific antibody titer

We first studied the VZV-specific immune status of all subjects by measuring serum antibody titers. As shown in Table 1, all healthy adults (subjects 1–3) had detectable anti-VZV IgG antibodies. Among the 12 children, including 3 infants, 4 (subjects 4, 5, 7, 8) had the antibodies, while the remaining 8 (subjects 6, 9–15) did not. For 7 of the 8 subjects without antibodies, there was no known history of chickenpox or varicella vaccination. For subject 6, the blood sample was drawn during the acute phase of varicella, and we did not detect anti-VZV IgM antibodies in this subject's blood.

3.2. Evaluation of VZV vaccine amounts in IR assay

We initially attempted the IR assay with a combination of 100 μ l of whole blood from 3 subjects (subjects 1–3) and various doses of varicella vaccine in a 24 h culture to assess whether this assay system was feasible. Whole blood produced IFN- γ with increasing amounts of vaccine from 10 to 50 μ l, but production of IFN- γ decreased at 100 μ l (Fig. 1). These results indicated that the IR assay system using whole blood and the vaccine preparation could be further investigated. Therefore, we subsequently performed the IR assays by culturing 100 μ l of whole blood with 50 μ l of vaccine and 50 μ l of RPMI 1640 medium per well.

Table 1
IgG antibody titers were estimated by the indirect immunofluorescence test and expressed as the highest dilution of serum showing a positive signal.

Subjects	Age	Antibody titer (IF)
1	32 Y	1:80
2	38 Y	1:40
3	28 Y	1:640
4	1 Y	>1:320
5	4 Y	1:80
6	2 Y	<1:10
7	2 Y	1:40
8	11 Y	1:80
9	3 Y	<1:10
10	11 M	<1:10
11	3 Y	<1:10
12	1 Y	<1:10
13	9 M	<1:10
14	10 M	<1:10
15	1 Y	<1:10

Y, years; M, months.

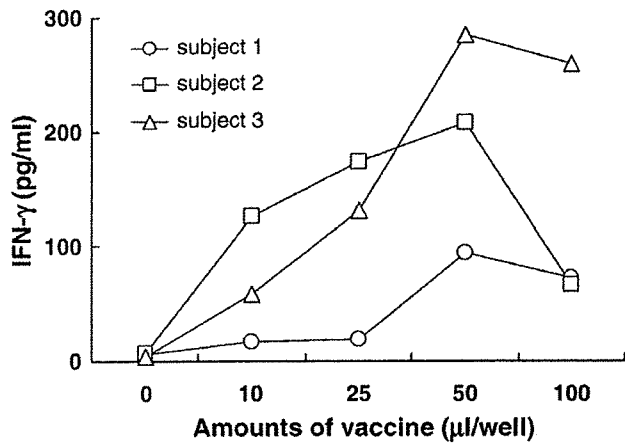


Fig. 1. Evaluation of VZV vaccine amounts suitable for IR assay. Various amounts of vaccine preparation, which were diluted 2 times and UV-irradiated, were mixed with 100 μl of whole blood in a final volume of 200 μl/well. Concentrations of IFN-γ in culture supernatants were measured 24 h later.

3.3. Evaluation of stability of whole blood

In a point-of-care setting, it may not be possible to perform the assay on whole blood samples immediately after collection. In order to investigate the functional stability of whole blood, samples were allowed to stand for 4 or 8 h at room temperature prior to the assay, and the production of IFN-γ in the 24-h cultures were compared with cultures of freshly isolated whole blood samples. After exposure to VZV, samples left standing for 4 h exhibited greater than or equal to 80% of the activity of fresh blood samples. However, blood samples from 2 subjects (1 and 3) lost 80% of their activity after being left standing for 8 h (Fig. 2A). After exposure to PHA, samples from all subjects were found to retain more than 60% activity after 4 h. However, almost all activity in samples from subjects 1 and 3 ceased after 8 h (Fig. 2B). These observations indicated that the assay should be performed on blood samples within 4 h of collection. Thus, all assays were performed within 1 h of obtaining blood samples.

3.4. Evaluation of culture time in IR assay

We next studied IFN-γ release over longer periods, i.e., 48 h, 72 h. As shown in Fig. 3, the amount of IFN-γ produced in the samples from all subjects in response to VZV increased over time, resulting in maximum production in the 72-h culture. However, in the samples of subjects 2 and 3, production almost reached maximum at 48 h. These results showed that whole blood must be cultured with the vaccine for at least 48 h to determine whether IFN-γ is released in response to VZV.

3.5. IR assay of blood from immune and non-immune subjects

Finally, we evaluated IFN-γ release among 12 subjects who had or did not have the anti-VZV antibody. In a 48-h culture of whole blood from 4 subjects who had anti-VZV antibodies (4, 5, 7, and 8) and from subject 6, who did not have antibodies, high amounts of IFN-γ were released. Blood from the remaining 7 subjects who had no antibodies (9–15) produced very low amounts of IFN-γ (Fig. 4). No increase in IFN-γ release was observed in blood from subjects 9–15, even after 72 h in culture

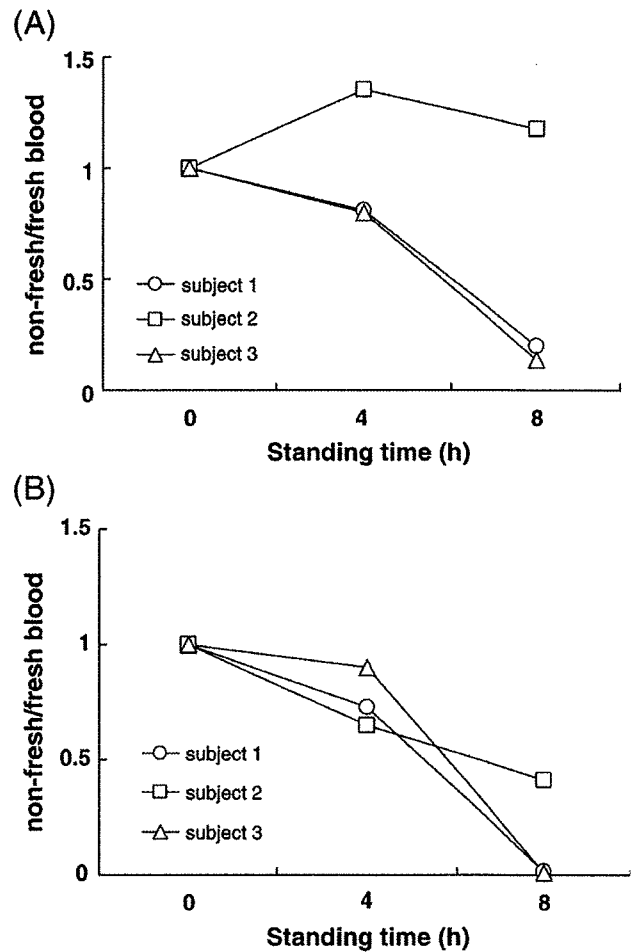


Fig. 2. Functional stability of whole blood samples for IFN-γ production. Freshly isolated whole blood samples from 3 subjects (1, 2, and 3) were kept at room temperature for 4 or 8 h. Whole blood samples (100 μl) were cultured with 100 μl of medium (negative control, NC) or vaccine (VZV), which contained 50 μl of vaccine preparation(A) or phytohemagglutinin (PHA; 5 μg/ml final)(B). Concentrations of IFN-γ in culture supernatants were measured 24 h later. The values were expressed as the ratio of IFN-γ released between freshly isolated blood and non-fresh blood.

(data not shown). When the levels of IFN-γ released and antibody titers of each subject were compared by calculating the correlation coefficient, no relation was observed at all.

4. Discussion

In this study, we assessed a new method that could simply and easily determine VZV-specific immunity. This method is easier to perform than other in vitro assays because the amount of IFN-γ produced in the culture supernatant can be directly determined following the incubation of the patient's whole blood with the commercially available VZV vaccine. Most importantly, we could clearly differentiate VZV-immune subjects from non-immune subjects by the level of IFN-γ production in their blood. Although further studies using a larger number of blood samples are needed, the results in Fig. 3 show that an IFN-γ level of over 100 pg/ml appears to indicate immunity against VZV. Because of its ability to induce Th1-dominant immunity, IFN-γ is considered to be a marker of CMI. Thus, the level of IFN-γ in the blood reflects the degree of

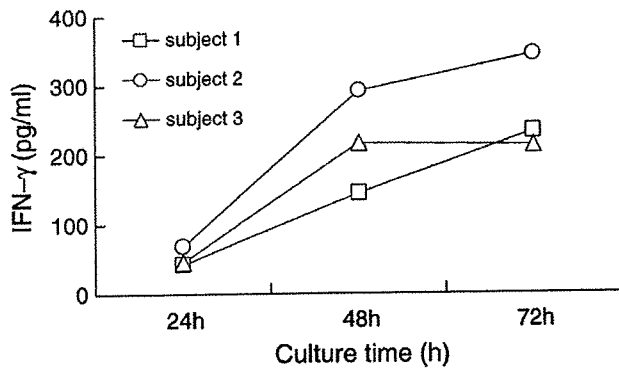


Fig. 3. IFN- γ production from the whole blood of 3 subjects after various culture times. IR assays were performed as described in the legend of Fig. 2, but culture supernatants were harvested after 48 h and 72 h of culture, in addition to the 24-h culture.

induction of CMI by the corresponding antigens. This principle was recently applied to confirm tuberculosis infection (Dinnes et al., 2007). Therefore, we concluded that subjects showing significant IFN- γ release in their blood (subjects 4–8) have CMI against VZV, but others (subjects 9–15) do not. Thus, the IR assay may be a candidate for measuring VZV-specific CMI in point-of-care settings.

Of particular interest are the observations for subject 6. The blood sample of this subject was drawn during the acute phase of the disease, and no antibodies against VZV, including IgM, were detected; however, a high level of IFN- γ release was observed. These findings indicate that the IR assay can detect early CMI response prior to antibody response, further indicating the utility of this method as a tool for early diagnosis.

The goal of measuring VZV-specific CMI is to predict the threshold level of immunity at which the reactivation of VZV cannot be prevented, thus causing HZ. However, to date the exact threshold value has not been determined. Levin et al. (2008) recently demonstrated an inverse correlation between the level of VZV-specific CMI and the likelihood of developing HZ by using the responder cell frequency (RCF) and ELISPOT assays. However, they did not identify a particular level of VZV-specific CMI, because of the small number of HZ cases in the study and an inability to collect samples during the onset of HZ. On the other hand, Hata et al. (2002) used the LP assay and reported intriguing observa-

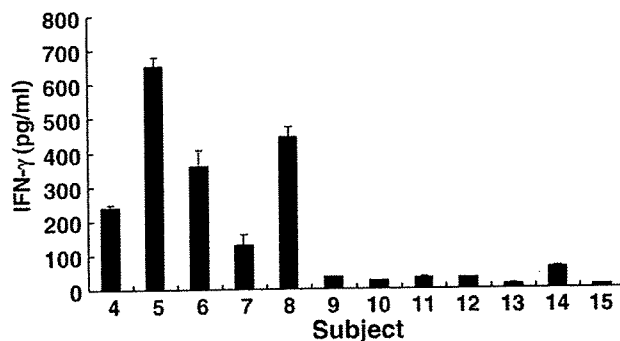


Fig. 4. IFN- γ production from the whole blood of 12 subjects. IR assays were performed as described in the legend of Fig. 2, but culture supernatants were harvested after 48 h.

tions in the analyses of patients who underwent hematopoietic-cell transplantation. They showed that the risk of HZ decreased for each unit increase above the stimulation index of 1.6; a stimulation index above 5.0 correlated with greater than 93% protection. As shown by Hata et al. (2002), monitoring VZV-specific CMI in patients with hematopoietic-cell transplantation would be a good experimental system to determine the threshold level of immunity.

In conclusion, we have developed a new assay that measures IFN- γ release induced by VZV antigens, that reflects VZV-specific CMI, and that correlates well to both history of varicella and the VZV-immune status of subjects. Therefore, the IR assay may be a good alternative for determining VZV-specific CMI.

References

- Arvin, A.M., Koropchak, C.M., 1980. Immunoglobulins M and G to varicella-zoster virus measured by solid-phase radioimmunoassay: antibody responses to varicella and herpes zoster infections. *J. Clin. Microbiol.* 12, 367.
- Arvin, A.M., Moffat, F., Redman, R., 1996. Varicella-zoster virus: aspects of pathogenesis and host response to natural infection and varicella vaccine. *Adv. Virus Res.* 46, 263.
- Dinnes, J., Deeks, J., Kunst, H., Gibson, A., Cummins, E., Waugh, N., Drobniewski, F., Lalvani, A., 2007. A systematic review of rapid diagnostic tests for the detection of tuberculosis infection. *Health Technol. Assess.* 11, 1.
- Gershon, A.A., LaRussa, P., Steinberg, S., 1996. The varicella vaccine. Clinical trials in immunocompromised individuals. *Infect. Dis. Clin. North Am.* 10, 583.
- Hata, A., Asanuma, H., Rinki, M., Sharp, M., Wong, R.M., Blume, K., Arvin, A.M., 2002. Use of an inactivated varicella vaccine in recipients of hematopoietic-cell transplants. *N. Engl. J. Med.* 347, 26.
- Levin, M.J., Smith, J.G., Kaufhold, R.M., Barber, D., Hayward, A.R., Chan, C.Y., Chan, I.S., Li, D.J., Wang, W., Keller, P.M., Shaw, A., Silber, J.L., Schlienger, K., Chalikhonda, I., Vessey, S.J., Caulfield, M.J., 2003. Decline in varicella-zoster virus (VZV)-specific cell-mediated immunity with increasing age and boosting with a high-dose VZV vaccine. *J. Infect. Dis.* 188, 1336.
- Levin, M.J., Oxman, M.N., Zang, J.H., Johnson, G.R., Stanley, H., Hayward, A.R., Caulfield, M.J., Irwin, M.R., Smith, J.G., Clair, J., Chan, I.S., Williams, H., Harbecke, R., Marchese, R., Straus, S.E., Gershon, A., Weinberg, A., 2008. Varicella-zoster virus-specific immune responses in elderly recipients of a herpes zoster vaccine. *J. Infect. Dis.* 197, 825.
- Meyers, J.D., Flournoy, N., Thomas, E.D., 1980. Cell-mediated immunity to varicella-zoster virus after allogeneic marrow transplant. *J. Infect. Dis.* 141, 479.
- Myers, M.G., 1979. Viremia caused by varicella-zoster virus: association with malignant progressive varicella. *J. Infect. Dis.* 140, 229.
- Oxman, M.N., Levin, M.J., Johnson, G.R., Schmader, K.E., Straus, S.E., Gelb, L.D., Arbeit, R.D., Simberkoff, M.S., Gershon, A.A., Davis, L.E., Weinberg, A., Boardman, K.D., Williams, H.M., Zhang, J.H., Peduzzi, P.N., Beisel, C.E., Morrison, V.A., Guatelli, J.C., Brooks, P.A., Kauffman, C.A., Pachucki, C.T., Neuzil, K.M., Betts, R.F., Wright, P.F., Griffin, M.R., Brunell, P., Soto, N.E., Marques, A.R., Keay, S.K., Goodman, R.P., Cotton, D.J., Gnann Jr., J.W., Loutit, J., Holodniy, M., Keitel, W.A., Crawford, G.E., Yeh, S.S., Lobo, Z., Toney, J.F., Greenberg, R.N., Keller, P.M., Harbecke, R., Hayward, A.R., Irwin, M.R., Kyriakides, T.C., Chan, C.Y., Chan, I.S., Wang, W.W., Annunziato, P.W., Silber, J.L., Shingles Prevention Study Group, 2005. A vaccine to prevent herpes zoster and postherpetic neuralgia in older adults. *N. Engl. J. Med.* 352, 2271–2284.
- Sartori, A.M., 2004. A review of the varicella vaccine in immunocompromised individuals. *Int. J. Infect. Dis.* 8, 259.
- Takahashi, M., Asano, Y., Kamiya, H., Baba, K., Ozaki, T., Otsuka, T., Yamanishi, K., 2008. Development of varicella vaccine. *J. Infect. Dis.* 197 (Suppl 2), S41.
- Webster, A., Grint, P., Brenner, M.K., Prentice, H.G., Griffiths, P.D., 1989. Titration of IgG antibodies against varicella zoster virus before bone marrow transplantation is not predictive of future zoster. *J. Med. Virol.* 27, 117.
- Wilson, A., Sharp, M., Koropchak, C.M., Ting, S.F., Arvin, A.M., 1992. Subclinical varicella-zoster virus viremia, herpes zoster, and T lymphocyte immunity to varicella-zoster viral antigens after bone marrow transplantation. *J. Infect. Dis.* 165, 119.
- Zaia, J.A., Levin, M.J., Preblud, S.R., Leszczynski, J., Wright, G.G., Ellis, R.J., 1983. Evaluation of varicella-zoster immune globulin: protection of immunosuppressed children after household exposure to varicella. *J. Infect. Dis.* 147, 737.
- Zhang, Y., Cosyns, M., Levin, M.J., Hayward, A.R., 1994. Cytokine production in varicella zoster virus-stimulated limiting dilution lymphocyte cultures. *Clin. Exp. Immunol.* 98, 128.

A First Total Synthesis of Ganglioside HLG-2**

Yuki Iwayama,^[a, b] Hiromune Ando,^{*[a, b]} Hideharu Ishida,^[c] and Makoto Kiso^{*[a, b]}

Abstract: A first synthesis of the neuritegenic ganglioside HLG-2, which was identified in extracts of the sea cucumber *Holothuria leucospilota*, is described. The characteristic sequence of the trisaccharide part, α -*N*-glycolylsialyl-(2,4)- α -*N*-acetylsialyl-(2,6)-glucoside, was efficiently assembled by coupling

of a highly active *N*-2,2,2-trichloroethoxycarbonyl (Troc)-protected sialyl donor and a 1,5-lactamized sialyl ac-

Keywords: gangliosides · glycolipids · natural products · sialic acids · total synthesis

ceptor with high stereoselectivity. The corresponding trisaccharyl imidate donor was directly glycosidated with the primary hydroxyl group of the ceramide part, producing protected HLG-2 in relatively high yield, global deprotection of which furnished ganglioside HLG-2 in highly pure form.

Introduction

Gangliosides, sialic acid-containing glycosphingolipids, have been attracting much attention due to their diverse biological functions. In mammals, gangliosides function as mediators for cell–cell recognition, virus–cell recognition, toxin–cell recognition, and cell signaling, and are also relevant to neural network formation, fertilization, and oncogenesis.^[1] The mammalian gangliosides, a family comprised of six major series (the hemato, ganglio, lacto, neolacto, globo, and isoglobo series), have been targeted by chemical synthetic studies over the last two decades. In our laboratory,

many gangliosides, such as sialyl Lewis X,^[2] GQ1b,^[3] and GQ1b α ,^[4] have been initially synthesized in a stereoselective and convergent manner, and then utilized in biological studies.^[5] Meanwhile, a variety of gangliosides have been isolated from echinoderms, and their unique structures have been characterized. To date, several series of echinodermatous gangliosides have been identified; for example, the LLG,^[6] HLG,^[7] AG,^[8] SJG,^[9] and LMG^[10] series. The attraction of echinodermatous gangliosides is that they show neuritegenic activity similar to that of mammalian gangliosides.^[11] However, their structure–activity relationships have yet to be delineated by using structurally homogeneous gangliosides.

Ganglioside HLG-2 is present in the sea cucumber *Holothuria leucospilota*, and was first isolated by Higuchi et al.^[7] Ganglioside HLG-2 showed neuritegenic activity toward the rat pheochromocytoma cell line PC-12 in the presence of nerve growth factor, and its activity was as potent as that of mammalian ganglioside GM1. As depicted in Figure 1, several unique structural features are present within the HLG-2 molecule. An α (2,4)-linkage between sialic acids is seen only in HLG series gangliosides (HLG-2 and HLG-3), and the tandem of *N*-glycolylsialic acid (NeuGc) and *N*-acetylsialic acid (NeuAc) is a further characteristic of HLG series gangliosides. In addition, the ceramide part in HLG-2 (**1** and **2**), which comprises a mammalian-type unsaturated sphingosine and an α -hydroxy fatty acid, is the sole combination among the echinodermatous gangliosides found to date. Compound **1** was isolated from *Holothuria leucospilota* as a major homologue of HLG-2.

Previously, our group embarked on new research concerning the systematic synthesis of echinodermatous gangliosides with a view to developing their potential as drug leads for

[a] Y. Iwayama, Dr. H. Ando, Dr. M. Kiso
Department of Applied Bioorganic Chemistry
Faculty of Applied Biological Sciences, Gifu University
1-1 Yanagido, Gifu-shi, Gifu 501-1193 (Japan)
E-mail: hando@gifu-u.ac.jp

[b] Y. Iwayama, Dr. H. Ando, Dr. M. Kiso
Institute for Integrated Cell-Material Sciences
Kyoto University
69 Konocho, Yoshida, Sakyo-ku, Kyoto 606-8501 (Japan)
Fax: (+81)58-293-3189

[c] Dr. H. Ishida
Department of Applied Bioorganic Chemistry
Faculty of Applied Biological Sciences, Gifu University
1-1 Yanagido, Gifu-shi, Gifu 501-1193 (Japan)

[**] Part 148 of the series: Synthetic studies on sialoglycoconjugates. For part 147, see: A. Imamura, H. Ando, H. Ishida, M. Kiso, *J. Org. Chem.* **2009**, in press.

Supporting information for this article is available on the WWW under <http://dx.doi.org/10.1002/chem.200802706>.

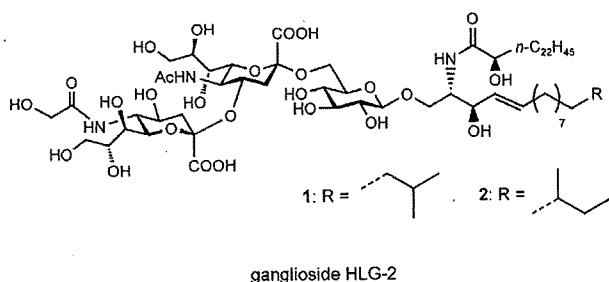


Figure 1. Ganglioside HLG-2.

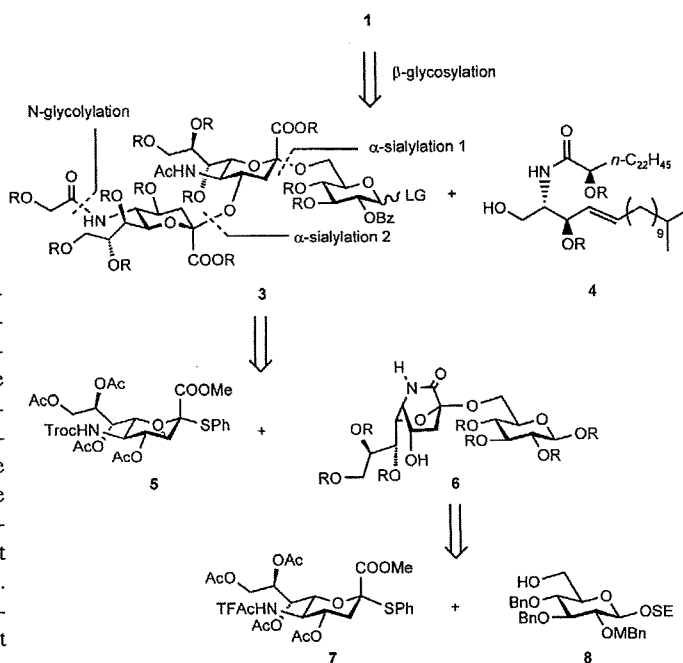
combatting neural disorders, and recently we reported a synthesis of the glycan part of HLG-2.^[12] In this paper, we describe in detail the first total synthesis of HLG-2.

Results and Discussion

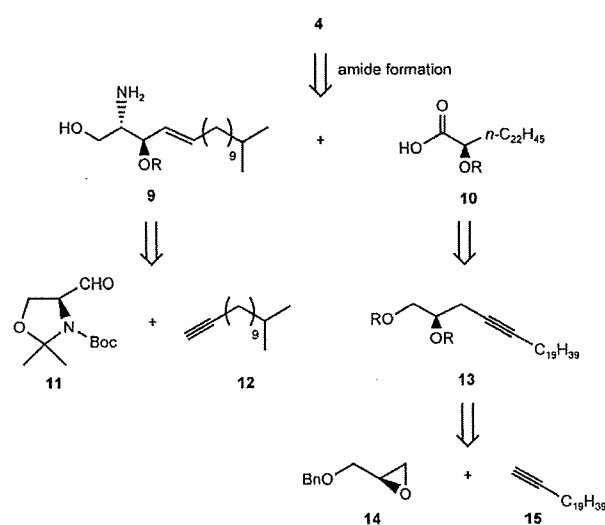
According to the literature on ganglioside synthesis, the conjugation of the glycan part with the ceramide may be conducted using several approaches. One major approach exploited the pre-incorporation of 2-azido-sphingosine at the reducing end of the glycan chain, which was followed by assembly of the ceramide structure.^[13] Alternatively, in another approach, the ceramide part was glycosylated with the full-length glycan part to directly fashion a ganglioside framework.^[14] Although this direct method tends to decrease the coupling yields of large ganglioside syntheses, it can offer high efficiency for small ganglioside syntheses. Therefore, our disconnection of target compound **1** gave trisaccharide glycosyl donor **3**, which bears a benzoyl group at C-2 of glucose as a β -directing functionality in glycosylation, and ceramide acceptor **4** (Scheme 1). The trisaccharide **3**, which has the sequence Neu5Gc- α (2,4)-Neu5Ac- α (2,6)-Glc, was further compartmentalized into *N*-2,2,2-trichloroethoxycarbonyl (Troc)-sialyl donor **5**^[15] and 1,5-lactamized sialyl glucosyl acceptor **6**,^[12] which is a linchpin to construct the Neu- α (2,4)-Neu tandem structure. To synthesize the lactamized sialyl glucosyl acceptor, *N*-trifluoroacetyl (TFAc) sialyl donor **7**^[16] and glucosyl acceptor **8** were chosen. To introduce the benzoyl group at the C-2 hydroxyl group of glucose after a basic lactamization reaction, the C-2 hydroxyl group was temporarily protected with the *p*-methoxybenzyl (MBn) group. The 2-(trimethylsilyl)ethyl (SE) group was chosen as a tentative aglycon during manipulation of the glycan part, based on our reported results of ganglioside syntheses.^[17]

On the other hand, the ceramide part was disconnected at the amide bond, affording (2*S*,3*R*)-2-amino-heptadec-4-ene-1,3-diol **9** and an α -hydroxy fatty acid **10**. According to an article by Murakami et al.,^[18] the coupling reaction of Garner's aldehyde **11**^[19] and alkyne **12** was expected to furnish a *trans*-alkene moiety within **9**. Fatty acid **10** was fragmented into oxirane **14** and alkyne **15** (Scheme 2).

In the synthesis of glucosyl acceptor **8**, we addressed the chemical discrimination in etherification of the C-2 and C-3 hydroxyl groups in 4,6-benzylidened glucoside **16**^[20] (Scheme 3). We first tried Hung's method (i) TMSCl, Et₃N; ii) Et₃SiH, PhCHO, TMSOTf.^[21] In the case of **16**, the 3-*O*-benzylated derivative **17** was generated in 61% yield and was accompanied by several unidentified by-products. In scaling-up this reaction, the generation of these unknown by-products could not be suppressed. Conversely, regioselective

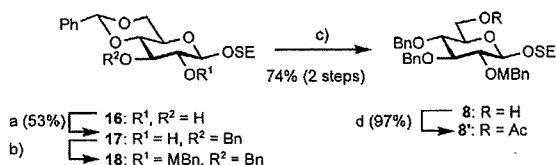


Scheme 1. Retrosynthetic analysis of the glycan part of **1**. SE = 2-(trimethylsilyl)ethyl, Bn = benzyl, MBn = *p*-methoxybenzyl.



Scheme 2. Retrosynthetic analysis of the ceramide part of **1**.

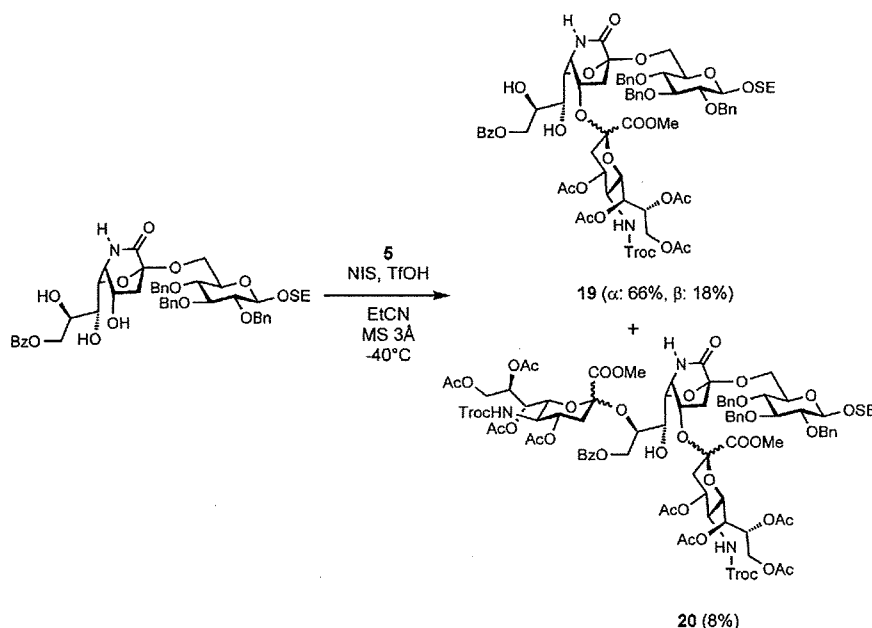
tive benzylation via the di-*n*-butylstannylidene intermediate^[22] afforded **17** in moderate yield (53%) on a large scale, concomitantly generating the 2-*O*-benzyl derivative in 34% yield. In view of the practicalities, the stannylidene-mediated benzylation was used for conversion to **17**. The C-2 hydroxyl group of **17** was protected with an MBn group in the conventional manner (MBnCl, NaH/DMF), and then the 4,6-benzylidene group was reductively opened upon treatment with DIBAL-H in toluene^[23] to yield the 6-OH glucosyl acceptor **8**. The position of the resulting free hydroxyl group was confirmed by NMR analysis of compound **8** and the corresponding acetylated derivative **8'**. Comparing **8'** and **8**, the signals of H-6a and H-6b were shifted to $\delta = 4.24$ and 4.34 ppm from $\delta = 3.71$ and 3.87 ppm, respectively.



Scheme 3. Synthesis of glucosyl acceptor **8**. a) i) *n*Bu₂SnO/PhMe, reflux, 8 h; ii) then, BnBr, *n*Bu₄NBr, reflux, 8 h, 53%; b) MBnCl, NaH/DMF, RT, 3 h; c) *i*Bu₂AlH/PhMe, RT, 18 h, 74% (2 steps); d) Ac₂O, py, RT, 15 h, 97%.

The assembly of the trisaccharide sequence of HLG-2 commenced with synthesis of the 1,5-lactam-sialyl glucosyl acceptor **25**. In our previous study on the synthesis of the HLG-2 glycan part,^[12] the corresponding 9-*O*-benzoyl-4,7,8-triol acceptor **19** was sialylated to yield the Neu- α (2,4)-Neu- α (2,6)-Glc sequence in 66% yield, along with the β -isomer (18%) and the Neu(2,8){Neu(2,4)}Neu(2,6)Glc tetrasaccharide **20** (8%) as a doubly-sialylated by-product (Scheme 4). In this study, to prevent the unwanted over-sialylation, the C-8 hydroxyl group was designed to be protected as an 8,9-*O*-isopropylidene (Scheme 5). The α -sialylation of the aforementioned glucosyl acceptor **8** with *N*-TFAc sialyl donor **7** was promoted by NIS/TfOH^[24] in MeCN/CH₂Cl₂ at -30°C to produce α -sialyl glucoside **21** in 75% yield along with β -isomer **22** (13%). The disaccharide was deacetylated by treatment with NaOMe in MeOH, and then 8,9-isopropylidenated by reaction with 2-dimethoxypropane and (\pm)-10-camphorsulfonic acid in MeCN to afford **24** in

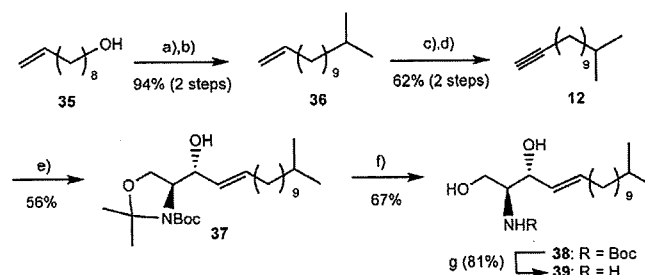
90% yield (over two steps). The position of the acetal was determined by comparison of the ¹H NMR chemical shifts of the H-7 signals of **24** and the corresponding acetylated derivative **24'**, similar to the case of compound **8**. Compound **24** was then converted into the 1,5-lactam form **25** in 95% yield by treatment with NaOMe in MeOH under reflux in the presence of Drierite as a drying agent. To our delight, the next sialylation of the diol acceptor **25** with *N*-Troc sialyl donor **5** occurred exclusively at the C-4 hydroxyl group in a stereoselective manner, delivering the HLG-2 glycan sequence **26** in 60% yield and the β -isomer **27** in 9% yield. As previously reported, the anomeric configurations of the new sialosides were determined on the basis of the coupling constant between C-1 and H-3_{ax} (**26**, ³J_{C1-H3ax} = 3.8 Hz; **27**, ³J_{C1-H3ax} < 1.0 Hz).^[25] The isolated **26** was then subjected to the reaction sequence for transformation to the trichloroacetimidate form **34** as a trisaccharide glycosyl donor. Thus, acid hydrolysis followed by conventional acetylation afforded **28**. To open the lactam moiety, the hydrogen of the lactam was substituted with a benzoyloxycarbonyl (Cbz) group by reaction with CbzOSu and DMAP, affording **29** in 79% yield. Prior to lactam opening, the MBn group at the C-3 position of glucose was selectively removed by treatment with DDQ and water,^[26] and this was followed by installment of the benzoyl group as a stereo-directing element in the final coupling reaction with the ceramide. Next, the Troc group of sialic acid was replaced with a benzylglycolyl group by subjecting **30** to reaction with Zn-Cu couple in AcOH,^[27] and this was followed by treatment with benzylglycolyl chloride to afford **31** in 89% yield over two steps. The lactam ring of **31** was then successfully hydrolyzed in a 7% triethylamine solution in MeCN/H₂O (9:5) at 40°C, and



Scheme 4. Previous result relating to assembly of the HLG-2 glycan framework.

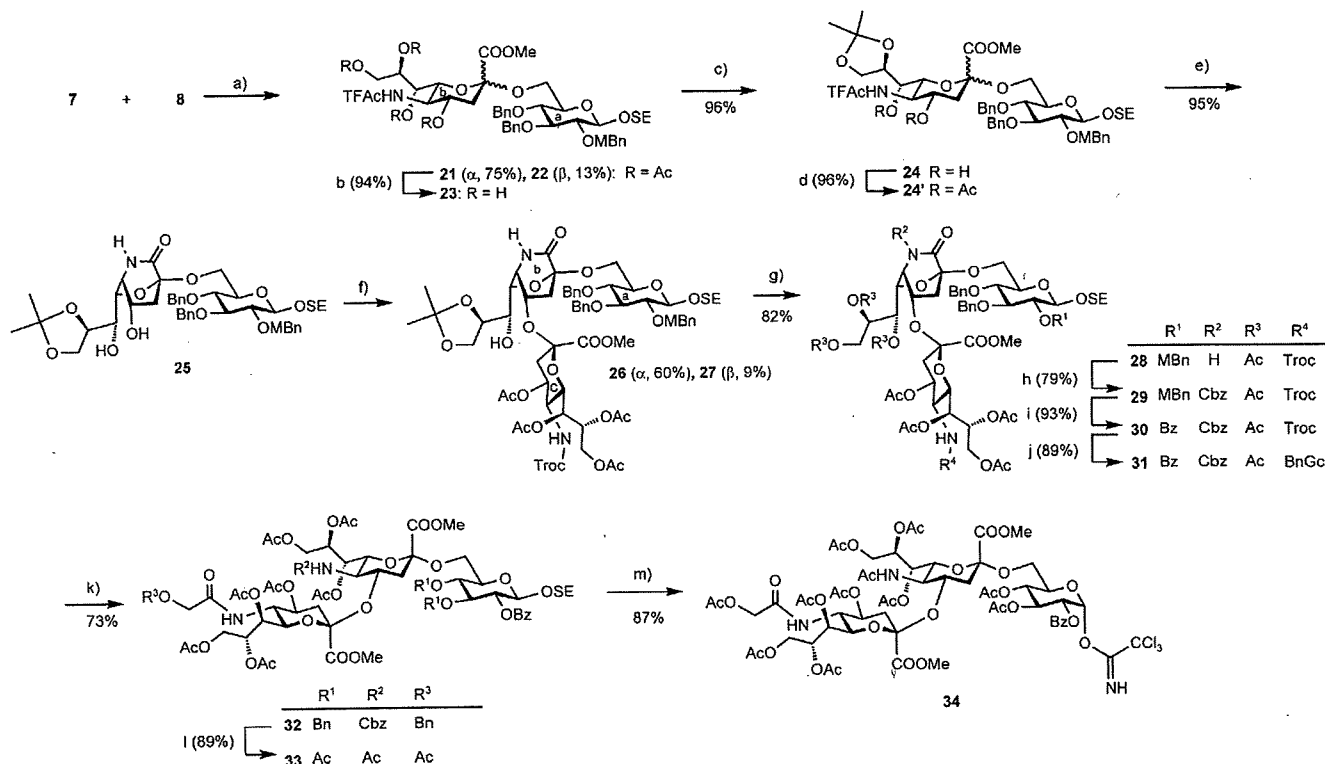
subsequent acetylation and methylation gave **32** in 73% yield (over three steps). The Cbz group and benzyl groups within **32** were hydrogenolyzed over Pd(OH)₂, and re-acetylation of the liberated amine and hydroxyl groups afforded the fully acylated trisaccharide **33**. Finally, treatment of **33** with trifluoroacetic acid in CH₂Cl₂ followed by reaction with CCl₃CN and DBU^[28] furnished the trisaccharide glycosyl donor **34**.

Starting from 9-decen-1-ol **35**, the known alkyne **12** was synthesized by the following procedures reported in the literature^[29] (Scheme 6). This conversion involved tosylation of the hydroxyl group of **35**, isobutylation with *i*BuMgBr and Li₂CuCl₄, and 1,2-dibromination followed by eliminative alkylation, thereby generating **12** in 58% yield over four steps. To assemble the *erythro*-sphingosine derivative, the alkyne **12** in hand was hydrozirconated by treatment with [Cp₂Zr(H)Cl], and subsequently reacted with Garner's aldehyde **11** in the presence of ZnBr₂ according to Murakami's method.^[18] This coupling reaction afforded *erythro*-sphingosine **37** in 56% yield, which was accompanied by unidentified by-products. The cyclic isopropylaminal was then re-



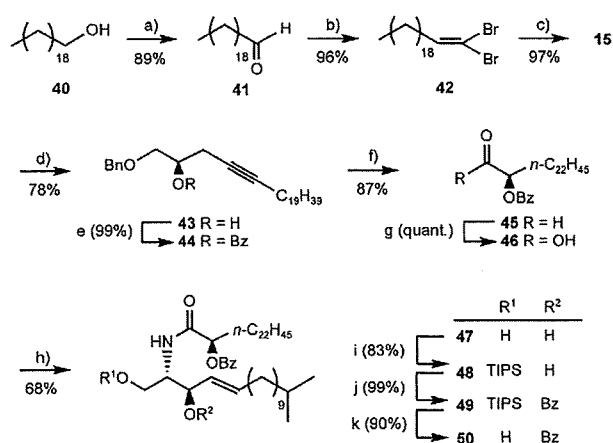
Scheme 6. Synthesis of sphingosine **39**. a) *p*-TsCl, py/CH₂Cl₂ 2:3, RT, 0°C, 2 h; b) *i*BuMgBr, Li₂CuCl₄/THF, -78°C→RT, 6 h, 94% (2 steps); c) Br₂/CH₂Cl₂, 0°C, 10 min; d) *t*BuOK, [18]crown-6/petroleum ether, reflux, 3 h, 62% (2 steps); e) i) [Cp₂Zr(H)Cl]/THF, RT, 1 h; ii) then **11**, ZnBr₂, RT, 18 h, 56%; f) 80% aq. AcOH, 45°C, 4 h, 67%; g) TFAcOH/CH₂Cl₂, RT, 15 min, 81%. Ts = tosyl, Cp = cyclopentadienyl.

moved in 80% aqueous AcOH and subsequent exposure to trifluoroacetic acid in CH₂Cl₂ yielded the unprotected sphingosine **39**, which was suitably predisposed for condensation with an incoming fatty acid.



Scheme 5. Synthesis of trisaccharide glycosyl donor **34**. a) NIS, TfOH, MS 3 Å, MeCN/CH₂Cl₂ 13:1, -30°C, 3.5 h, 88% (α/β 75:13); b) **21**, NaOMe, MeOH, RT, 2 h, 94%; c) DMP, CSA/MeCN, RT, 2 h, 96%; d) Ac₂O, py, RT, 2 h, 96%; e) NaOMe, Drierite/MeOH, reflux, 92 h, 95%; f) **5**, NIS, TfOH, MS 3 Å, EtCN/CH₂Cl₂ 9:1, -40°C, 16 h, 69% (α/β 60:9); g) i) **26**, 80% aq. AcOH, 45°C, 17 h; ii) Ac₂O, py, RT, 6 h, 82% (2 steps); h) CbzOSu, DMAP/py, RT, 48 h, 79%; i) i) DDQ, H₂O/CH₂Cl₂, RT, 2 h; ii) Bz₂O, DMAP/py, RT, 20 h, 93% (2 steps); j) i) Zn-Cu/AcOH, RT, 45 min; ii) BnGcCl/THF, 1.5 h, 89% (2 steps); k) i) 10% Et₃N solution in MeCN/H₂O 2:1, 40°C, 19 h; ii) Ac₂O, DMAP/py, RT, 1 h; iii) MeI, K₂CO₃/DMF, RT, 1 h, 73% (3 steps); l) i) H₂, Pd(OH)₂, AcOH, EtOH/THF (3:1), RT, 1 h; ii) Ac₂O, DMAP/py, RT, 6.5 h, 89% (2 steps); m) i) TFA/CH₂Cl₂, RT, 4 h; ii) CCl₃CN, DBU/CH₂Cl₂, 0°C, 1 h, 87% (2 steps). NIS = *N*-iodosuccinimide, TfOH = trifluoromethanesulfonic acid, MS = molecular sieves, DMP = 2,2-dimethoxypropane, CSA = (±)-10-camphorsulfonic acid, Cbz = benzyloxycarbonyl, DMAP = 4-dimethylaminopyridine, DDQ = 2,3-dichloro-5,6-dicyano-*p*-benzoquinone, Bz = benzoyl, Gc = glycolyl, TFA = trifluoroacetic acid, TFAc = trifluoroacetyl, DBU = 1,8-diazabicyclo[5.4.0]undec-7-ene.

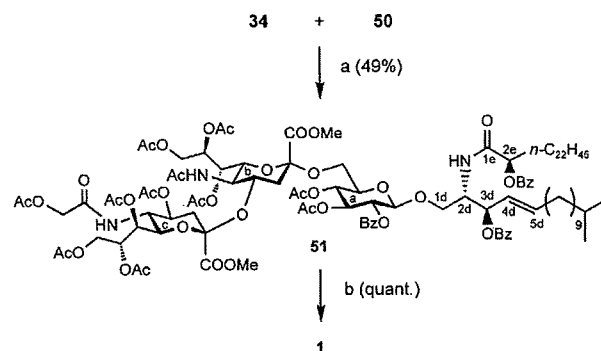
The synthesis of (*R*)-2-hydroxytetracosanoic acid derivative **46** commenced with the conversion of 1-icosanol **40** into heneicos-1-yne **15** (Scheme 7). Although Komori et al. have previously reported a synthesis of **15**,^[30] which involved coupling of 1-heptyne and 1-bromotetradecane and migration of the triple bond, we were unable to reproduce their reported yields for each reaction step. In this study, therefore, we designed an alkyne moiety by the Corey–Fuchs approach.^[31] Thus, 1-icosanol **40** was first converted into aldehyde **41** in 89% yield by Dess–Martin oxidation.^[32] One-carbon-extension of **41** by reaction with CBr₄ and PPh₃ yielded dibromoalkene **42**, treatment of which with *n*BuLi in THF at –78 °C afforded the terminal acetylene **15** in pure form and in almost quantitative yield (93% over two steps). Alkylation of **15** with the commercially available oxirane **14** was conducted according to an earlier report by Komori et al.,^[30] affording **43** in 78% yield. The secondary hydroxyl group of **43** was protected with a benzoyl group, and hydrogenolysis of the benzyl group and the triple bond, followed by Dess–Martin oxidation, afforded α -benzyloxy aldehyde **45** in 87% yield over two steps. The aldehyde **45** was then oxidized to the carboxylic acid by the action of NaClO₂ in the presence of 2-methyl-2-butene^[33] to quantitatively afford the desired α -hydroxy fatty acid **46**. The synthesized fatty acid **46** and the aforementioned sphingosine **39** were coupled under catalysis by 1-ethyl-3-(dimethylaminopropyl)carbodiimide hydrochloride in CH₂Cl₂, producing ceramide framework **47** in 68% yield. The primary hydroxyl group at C-1 was selectively protected as triisopropylsilyl (TIPS)



Scheme 7. Synthesis of ceramide acceptor **50**. a) Dess–Martin periodinane, NaHCO₃/CH₂Cl₂, RT, 1 h, 89%; b) CBr₄, PPh₃/CH₂Cl₂, 0 °C → RT, 2 h, 96%; c) *n*BuLi/THF, –78 °C → RT, 1 h, 97%; d) **14**, *n*BuLi, HMPA/THF, RT, 2.5 h, 78%; e) BzCl, DMAP/py, RT, 2 h, 99%; f) i) H₂, Pd(OH)₂/EtOH, RT, 1.5 h; ii) Dess–Martin periodinane, NaHCO₃/CH₂Cl₂, RT, 1 h, 87% (2 steps); g) NaClO₂, NaH₂PO₄, 2-methyl-2-butene, *t*BuOH/THF/H₂O (5:4:1), 30 °C, 15 min, quant.; h) **39**, EDCI-HCl/CH₂Cl₂, RT, 18 h, 68%; i) TIPSCl, imidazole/DMF, RT, 2.5 h, 83%; j) Bz₂O, DMAP/py, 17 h, 99%; k) TBAF, AcOH/THF, RT, 24 h, 90%. HMPA = hexamethylphosphoric triamide, EDCI = 1-ethyl-3-(3-dimethylaminopropyl)carbodiimide, TIPS = triisopropylsilyl, TBAF = tetra-*n*-butylammonium fluoride.

ether, allowing benzylation of the remaining unprotected hydroxyl group. Finally, the TIPS group was removed by the action of TBAF in the presence of AcOH in THF, furnishing ceramide acceptor **50**.

As depicted in Scheme 8, coupling of the trisaccharide glycosyl donor **34** (1.0 equiv) with the ceramide acceptor **50** (1.3 equiv), which was promoted by TMSOTf (0.8 equiv in total), successfully afforded protected HLG-2 **51** in 49% yield. Finally, global deprotection of **51** delivered ganglioside HLG-2 **1**.



Scheme 8. Assembly of the fully protected HLG-2 and its deprotection. a) TMSOTf, AW-300/CH₂Cl₂, 0 °C → 10 °C → RT, 17.5 h, 49%; b) i) NaOMe, MeOH, RT, 4 h; ii) then H₂O, RT, 116 h, quant. TMSOTf = trimethylsilyl trifluoromethanesulfonate, AW-300 = acid-washed 4 Å molecular sieves.

In summary, we have presented the first synthesis of ganglioside HLG-2. In the assembly of the glycan part, NeuGc- α (2,4)-NeuAc- α (2,6)-Glc, the yield of the sialylation at the C-4 hydroxyl group of the sialic acid residue was improved by exploiting the 8,9-isopropylidenedated 1,5-lactam-sialyl unit as a novel glycosyl acceptor. The three chiral carbons of the ceramide part were each efficiently established in a stereo-selective manner. The final connection of the glycan and ceramide parts was accomplished with relatively high yield. We are now investigating the neuritegenic activity of synthetic HLG-2 toward the PC-12 and Neuro2a cell lines.

Experimental Section

General procedures: ¹H and ¹³C NMR spectra were recorded with Varian Unity INOVA 400, INOVA 500, JEOL JNM-ECX400P, JNM-ECA500, and JNM-ECA600 spectrometers. Chemical shifts are expressed in ppm (δ) relative to the signal of Me₄Si as an internal standard. High-resolution mass spectrometry (HRMS) was performed with a Bruker Daltonics micrOTOF (ESI-TOF) mass spectrometer. FAB mass spectra were recorded on a JEOL JMS-700/GI using *m*-nitrobenzyl alcohol (NBA) as a matrix. MALDI-TOF mass spectra were recorded on a Bruker Autoflex using α -cyano-4-hydroxy-cinnamic acid (CHCA) as a matrix. Specific rotations were determined with a Horiba SEPA-300 high-sensitivity polarimeter. Molecular sieves were purchased from Wako Chemicals Inc. and dried at 300 °C for 2 h in a muffle furnace prior to use. Drierite was powdered and dried at 300 °C for 6 h in a muffle furnace prior to use. Solvents as reaction media were dried over molecular sieves and used with-

out further purification. TLC analysis was performed on Merck TLC plates (silica gel 60F₂₅₄ on glass). Compounds were visualized either by exposure to UV light (254 nm) or by spraying with 10% H₂SO₄ solution in EtOH, 20% phosphomolybdic acid solution in EtOH, or ninhydrin reagent, followed by heating. Flash column chromatography on silica gel (Fuji Silysia Co., 80 mesh and 300 mesh) or Sephadex (Pharmacia LH-20) was performed with the solvent systems (v/v) specified. Evaporation and concentration were conducted in vacuo.

2-(Trimethylsilyl)ethyl 3,4-di-*O*-benzyl-2-*O*-*p*-methoxybenzyl-β-*D*-glucopyranoside (8): NaH (60% dispersion in mineral oil; 971 mg, 24.3 mmol) was added to a solution of compound 17 (5.57 g, 12.1 mmol) in DMF (121 mL) and the mixture was stirred for 40 min at 0°C. *p*-Methoxybenzyl chloride (1.82 mL, 13.4 mmol) was then added and stirring was continued for 3 h at room temperature. Completion of the reaction was confirmed by TLC (hexane/EtOAc 3:1). The reaction mixture was then quenched with EtOH and saturated aqueous NH₄Cl solution at 0°C, and extracted with EtOAc. The organic layer was washed sequentially with water and brine, dried over Na₂SO₄, and concentrated. The residue was roughly purified by column chromatography on silica gel (hexane/EtOAc 12:1) to give crude 18 (7.37 g). The crude material was dried for 21 h and then dissolved in toluene (160 mL), and the resulting solution was cooled to 0°C. DIBAL-H (1.5 M solution in toluene; 20.2 mL, 30.3 mmol) was added and the resulting mixture was stirred for 18 h at room temperature. Completion of the reaction was confirmed by TLC (hexane/EtOAc 3:1). After the addition of Rochelle salt {KOOCC(OH)-CH(OH)-COONa}, the suspension was extracted with EtOAc. The organic layer was washed with brine, dried over Na₂SO₄, and concentrated. The residue was purified by column chromatography on silica gel (hexane/EtOAc 5:1) to give 8 (5.21 g, 74%). [α]_D²⁰ = +14.0° (c = 3.1, CHCl₃); ¹H NMR (500 MHz, CDCl₃): δ = 7.50–6.82 (m, 14H; 3 Ar), 4.94–4.62 (d, 6H; ArCH₂), 4.43 (d, 1H, J_{1,2} = 7.8 Hz; H-1), 3.99 (m, 1H; TMSCH₂CH₂), 3.87 (m, 1H; H-6), 3.75 (s, 3H; OMe), 3.71 (m, 1H; H-6'), 3.63 (m, 2H; H-3, TMSCH₂CH₂), 3.59 (app t, 1H, J_{3,4} = 9.3, J_{4,5} = 9.5 Hz; H-4), 3.39 (dd, 1H, J_{2,3} = 9.0 Hz; H-2), 3.35 (m, 1H; H-5), 1.05 ppm (m, 2H; TMSCH₂CH₂); ¹³C NMR (100 MHz, CDCl₃): δ = 159.2, 138.6, 138.0, 130.6, 129.8, 128.5, 128.1, 127.9, 127.8, 127.6, 113.8, 103.3, 84.5, 82.1, 77.2, 75.6, 75.1, 74.9, 74.5, 67.8, 62.1, 55.2, 18.7, 14.2, –1.4 ppm; HRMS: *m/z*: calcd for C₃₃H₄₄O₇Si + Na⁺: 603.2754 [M+Na]⁺; found: 603.2774.

2-(Trimethylsilyl)ethyl 6-*O*-acetyl-3,4-di-*O*-benzyl-2-*O*-*p*-methoxybenzyl-β-*D*-glucopyranoside (8'): Acetic anhydride (500 μL) was added to a solution of compound 8 (124 mg, 214 μmol) in pyridine (800 μL). The mixture was stirred for 15 h at room temperature. Completion of the reaction was confirmed by TLC (hexane/EtOAc 4:1). The reaction mixture was then concentrated and the residual solvent was removed by co-evaporation with toluene. The residue was purified by column chromatography on silica gel (hexane/EtOAc 7:1) to give 8' (129 mg, 97%). [α]_D²⁰ = –20.0° (c = 1.2, CHCl₃); ¹H NMR (500 MHz, CDCl₃): δ = 7.34–6.82 (m, 14H; 3 Ar), 4.97–4.54 (d, 6H; ArCH₂), 4.40 (d, 1H, J_{1,2} = 8.0 Hz; H-1), 4.33 (d, 1H, J_{gem} = 12.0 Hz; H-6), 4.24 (dd, 1H, J_{5,6} = 4.6 Hz; H-6'), 3.99 (m, 1H; TMSCH₂CH₂), 3.76 (s, 3H; OMe), 3.63 (m, 2H; H-3, TMSCH₂CH₂), 3.51 (m, 2H; H-4, H-5), 3.43 (app t, 1H, J_{2,3} = 8.6 Hz; H-2), 2.02 (s, 3H; Ac), 1.07 ppm (m, 2H; TMSCH₂CH₂); ¹³C NMR (100 MHz, CDCl₃): δ = 170.6, 159.1, 138.4, 137.7, 130.5, 129.7, 128.4, 128.3, 128.0, 127.8, 127.7, 127.5, 113.7, 103.1, 84.6, 81.8, 77.4, 75.5, 74.9, 74.3, 72.6, 67.5, 63.1, 55.1, 20.7, 18.4, –1.5 ppm; HRMS: *m/z*: calcd for C₃₅H₄₆O₈Si + Na⁺: 645.2860 [M+Na]⁺; found: 645.2884.

2-(Trimethylsilyl)ethyl (methyl 4,7,8,9-tetra-*O*-acetyl-3,5-dideoxy-5-trifluoroacetamido-*D*-glycero-α-*D*-galacto-2-nonulopyranosylonate)-(2→6)-3,4-di-*O*-benzyl-2-*O*-*p*-methoxybenzyl-β-*D*-glucopyranoside (21) and β-isomer (22): 3 Å molecular sieves (8.0 g) were added to a solution of compounds 7 (3.05 g, 4.78 mmol) and 8 (2.22 g, 3.82 mmol) in MeCN (43 mL)/CH₂Cl₂ (3.3 mL). The suspension was stirred for 1 h at room temperature and then cooled to –30°C, whereupon *N*-iodosuccinimide (NIS) (1.70 g, 7.17 mmol) and trifluoromethanesulfonic acid (TfOH) (42 μL, 478 μmol) were added. Stirring was continued for 3.5 h, after which TLC analysis (PhMe/acetone 4:1) indicated completion of the reaction. The reaction mixture was made alkaline to pH 8 with saturated

aqueous NaHCO₃ solution at 0°C, filtered through Celite, and the filter bed was washed with EtOAc. The combined filtrate and washings were extracted with EtOAc, and the organic layer was washed with saturated aqueous Na₂S₂O₃ and brine, dried over Na₂SO₄, and concentrated. The residue was purified by column chromatography on silica gel (CHCl₃/EtOAc 8:1→7:1) to give 21 (3.20 g, 75%) and 22 (541 mg, 13%). 21: [α]_D²⁰ = –1.1° (c = 1.4, CHCl₃); ¹H NMR (500 MHz, CDCl₃): δ = 7.33–6.82 (m, 14H; 3 Ar), 6.17 (d, 1H, J_{NH,5} = 10.0 Hz; NH), 5.41 (m, 1H; H-8b), 5.26 (dd, 1H, J_{6,7} = 2.2, J_{7,8} = 9.3 Hz; H-7b), 4.99 (m, 1H; H-4b), 4.89–4.64 (d, 6H; ArCH₂), 4.34 (d, 1H, J_{1,2} = 8.1 Hz; H-1a), 4.23 (dd, 1H, J_{5,6} = 10.7 Hz; H-6b), 4.17 (m, 2H; H-4a, H-9b), 3.95 (m, 3H; H-5b, H-9'b, TMSCH₂CH₂), 3.79 (s, 3H; OMe), 3.76 (s, 3H; COOMe), 3.59 (m, 4H; H-3a, H-6a, H-6'a, TMSCH₂CH₂), 3.38 (m, 2H; H-2a, H-5a), 2.72 (dd, 1H, J_{gem} = 12.7, J_{3,eq,4} = 4.6 Hz; H-3b_{eq}), 2.14–1.91 (m, 13H; H-3b_{ax}, 4 Ac), 1.04 ppm (m, 2H; TMSCH₂CH₂); ¹³C NMR (100 MHz, CDCl₃): δ = 170.9, 170.5, 170.1, 169.8, 167.7, 159.1, 157.7, 157.3, 138.7, 138.4, 130.7, 129.7, 128.3, 128.2, 127.9, 127.7, 127.5, 116.8, 114.0, 113.7, 103.1, 98.8, 84.5, 81.8, 77.4, 75.6, 74.8, 74.3, 73.7, 71.5, 68.5, 67.3, 66.9, 63.9, 61.9, 55.2, 52.6, 50.1, 37.9, 29.6, 20.6, 20.5, 20.3, 18.5, –1.5 ppm; HRMS: *m/z*: calcd for C₅₃H₆₈F₃NO₁₉Si + Na⁺: 1130.4005 [M+Na]⁺; found: 1130.4020. 22: [α]_D²⁰ = +1.5° (c = 1.3, CHCl₃); ¹H NMR (500 MHz, CDCl₃): δ = 7.33–6.84 (m, 14H; 3 Ar), 6.73 (d, 1H, J_{NH,5} = 10.3 Hz; NH), 5.41 (m, 1H; H-8b), 5.29 (dd, 1H, J_{6,7} = 2.3, J_{7,8} = 4.0 Hz; H-7b), 5.29 (m, 1H; H-8b), 4.94–4.66 (m, 7H; H-9b, ArCH₂), 4.59 (dd, 1H, J_{5,6} = 10.3 Hz; H-6b), 4.45 (d, 1H, J_{1,2} = 8.0 Hz; H-1a), 4.14 (m, 2H; H-5b, H-9'b), 4.04 (m, 1H; TMSCH₂CH₂), 3.75 (m, 10H; H-4a, H-6a, H-6'a, COOMe, OMe, TMSCH₂CH₂), 3.61 (app t, J_{2,3} = 9.2, J_{3,4} = 9.7 Hz; H-3a), 3.45 (m, 2H; H-2a, H-5a), 2.43 (dd, 1H, J_{gem} = 12.6, J_{3,eq,4} = 4.6 Hz; H-3b_{eq}), 2.18–2.00 (m, 12H; 4Ac), 1.96 (app t, 1H; H-3b_{ax}), 1.07 ppm (m, 2H; TMSCH₂CH₂); ¹³C NMR (125 MHz, CDCl₃): δ = 170.6, 170.5, 169.9, 169.7, 166.8, 159.2, 157.8, 157.6, 138.5, 138.2, 130.5, 129.8, 128.4, 128.3, 127.8, 127.8, 127.7, 127.6, 116.6, 114.3, 113.8, 103.2, 97.5, 84.1, 82.0, 76.4, 75.7, 75.0, 74.8, 73.5, 71.3, 70.2, 68.6, 68.3, 68.0, 62.4, 60.9, 55.2, 52.7, 49.6, 37.1, 20.7, 20.6, 20.6, 18.6, –1.6 ppm; HRMS: *m/z*: calcd for C₅₃H₆₈F₃NO₁₉Si + Na⁺: 1130.4005 [M+Na]⁺; found: 1130.4004.

2-(Trimethylsilyl)ethyl (methyl 3,5-dideoxy-5-trifluoroacetamido-*D*-glycero-α-*D*-galacto-2-nonulopyranosylonate)-(2→6)-3,4-di-*O*-benzyl-2-*O*-*p*-methoxybenzyl-β-*D*-glucopyranoside (23): A 28% solution of sodium methoxide (59 mg, 306 μmol) in MeOH was added to a solution of compound 21 (2.76 g, 2.49 mmol) in MeOH (36 mL). The mixture was stirred for 2 h at room temperature, and the progress of the reaction was monitored by TLC (CHCl₃/MeOH 10:1). The reaction mixture was then neutralized with Dowex-50 (H⁺), filtered, and concentrated. The residue was purified by column chromatography on silica gel (CHCl₃/MeOH 38:1→20:1) to give 23 (2.19 g, 94%). [α]_D²⁰ = –0.2° (c = 1.0, CHCl₃/MeOH 1:1); ¹H NMR (500 MHz, CD₃OD): δ = 7.31–6.80 (m, 14H; 3 Ar), 4.86–4.61 (d, 6H; ArCH₂), 4.39 (d, 1H, J_{1,2} = 7.8 Hz; H-1a), 3.99 (m, 2H; H-5b, TMSCH₂CH₂), 3.79 (m, 12H; H-6a, H-4b, H-6b, H-7b, H-8b, H-9b, COOMe, OMe), 3.63 (m, 2H; H-9'b, TMSCH₂CH₂), 3.57 (app t, 1H, J_{2,3} = 9.0, J_{3,4} = 8.8 Hz; H-3a), 3.50 (m, 2H; H-4a, H-6'a), 3.40 (m, 1H; H-5a), 3.29 (m, 1H; H-2a), 2.75 (dd, 1H, J_{gem} = 12.9, J_{3,eq,4} = 4.6 Hz; H-3b_{eq}), 1.80 (app t, 1H; H-3b_{ax}), 1.02 ppm (m, 2H; TMSCH₂CH₂); ¹³C NMR (100 MHz, CD₃OD): δ = 170.5, 160.7, 140.0, 139.7, 132.0, 130.7, 129.3, 129.1, 128.8, 128.7, 128.5, 114.6, 104.2, 100.3, 85.8, 83.1, 78.8, 76.5, 75.8, 75.3, 75.1, 73.9, 72.6, 70.0, 68.4, 64.5, 64.3, 55.7, 53.9, 53.4, 41.7, 19.4, –1.3 ppm; HRMS: *m/z*: calcd for C₄₅H₆₀F₃NO₁₅Si + Na⁺: 962.3582 [M+Na]⁺; found: 962.3580.

2-(Trimethylsilyl)ethyl (methyl 3,5-dideoxy-8,9-*O*-isopropylidene-5-trifluoroacetamido-*D*-glycero-α-*D*-galacto-2-nonulopyranosylonate)-(2→6)-3,4-di-*O*-benzyl-2-*O*-*p*-methoxybenzyl-β-*D*-glucopyranoside (24): 2,2-Dimethoxypropane (193 μL, 1.57 mmol) and (±)-10-camphorsulfonic acid (12 mg, 52 μmol) were added to a solution of compound 23 (981 mg, 1.04 mmol) in MeCN (20.8 mL). The mixture was stirred for 2 h at room temperature, and the progress of the reaction was monitored by TLC (hexane/EtOAc 1:1). The reaction mixture was then made alkaline to pH 9 with triethylamine and the volatiles were co-evaporated with toluene. The residue was subjected to column chromatography on silica gel (hexane/EtOAc 7:3) to give 24 (982 mg, 96%). [α]_D²⁰ = +0.3° (c = 1.5, CHCl₃); ¹H NMR (500 MHz, CD₃OD): δ = 7.33–6.81 (m, 14H; 3 Ar),

4.88–4.62 (6 d, 6H; ArCH₂), 4.40 (d, 1H, $J_{1,2}$ =7.8 Hz; H-1a), 4.21 (q, 1H; H-6b), 3.97 (m, 5H; H-6a, H-5b, H-8b, TMSCH₂CH₂), 3.78 (m, 9H; H-4b, H-9b, H-9'b, COOMe, OMe), 3.65 (m, 1H; TMSCH₂CH₂), 3.59 (app t, 1H, $J_{2,3}$ =9.0, $J_{3,4}$ =8.8 Hz; H-3a), 3.53 (app d, 1H; H-7b), 3.49 (app t, 1H, $J_{4,5}$ =9.8 Hz; H-4a), 3.42 (m, 1H; H-6'a), 3.31 (m, 2H; H-2a, H-5a), 2.72 (dd, 1H, J_{gem} =12.7, $J_{3eq,4}$ =4.6 Hz; H-3b_{eq}), 1.77 (app t, 1H; H-3b_{ax}), 1.34–1.29 (2 s, 6H; 2 Me), 1.02 ppm (m, 2H; TMSCH₂CH₂); ¹³C NMR (100 MHz, CDCl₃): δ = 168.4, 159.2, 158.7, 158.3, 138.5, 138.1, 130.6, 129.7, 128.4, 128.3, 127.9, 127.8, 127.6, 117.0, 114.1, 113.8, 108.9, 103.1, 99.0, 84.6, 81.9, 77.6, 75.6, 75.5, 74.8, 74.4, 73.9, 72.6, 69.9, 67.7, 67.1, 66.4, 63.6, 55.2, 53.9, 52.5, 39.9, 26.7, 25.5, 18.5, –1.5 ppm; HRMS: *m/z*: calcd for C₄₈H₆₄F₃NO₁₅Si + Na⁺: 1002.3895 [M+Na]⁺; found: 1002.3837.

2-(Trimethylsilyl)ethyl (methyl 4,7-di-O-acetyl-3,5-dideoxy-8,9-O-isopropylidene-5-trifluoroacetamido-D-glycero-α-D-galacto-2-nonulopyranosylonate)-(2→6)-3,4-di-O-benzyl-2-O-p-methoxybenzyl-β-D-glucopyranoside (24): Acetic anhydride (500 μL) was added to a solution of compound 24 (54.0 mg, 55.1 μmol) in pyridine (1.0 mL) and the mixture was stirred for 2 h at room temperature. Completion of the reaction was confirmed by TLC (hexane/EtOAc 1:1), whereupon the reaction mixture was concentrated and residual volatiles were removed by co-evaporation with toluene. The residue was purified by column chromatography on silica gel (CHCl₃/EtOAc 3:1) to give 24⁺ (56.1 mg, 96%). [α]_D = 2.4° (*c* = 1.8, CHCl₃); ¹H NMR (600 MHz, CDCl₃): δ = 7.34–6.82 (m, 14H; 3 Ar), 6.23 (brd, 1H; NH), 5.26 (dd, 1H, $J_{6,7}$ =2.1, $J_{7,8}$ =4.8 Hz; H-7b), 5.09 (m, 1H; H-4b), 4.91–4.64 (6 d, 6H; ArCH₂), 4.34 (m, 2H; H-1a, H-8b), 3.95 (m, 6H; H-6a, H-5b, H-6b, H-9b, H-9'b, TMSCH₂CH₂), 3.78 (2 s, 6H; COOMe, OMe), 3.59 (m, 3H; H-3a, H-4a, TMSCH₂CH₂), 3.37 (m, 2H; H-2a, H-5a), 2.74 (dd, 1H, J_{gem} =13.1, $J_{3eq,4}$ =4.8 Hz; H-3b_{eq}), 2.02–1.99 (2 s, 6H; 2 Ac), 1.90 (app t, 1H; H-3b_{ax}), 1.34–1.32 (2 s, 6H; 2 Me), 1.04 ppm (m, 2H; TMSCH₂CH₂); ¹³C NMR (125 MHz, CDCl₃): δ = 170.8, 170.2, 167.6, 159.2, 138.6, 138.2, 138.1, 130.6, 129.8, 128.5, 128.4, 128.3, 128.0, 127.9, 127.8, 127.6, 113.7, 108.7, 103.1, 99.1, 84.6, 81.8, 77.4, 75.6, 75.3, 75.1, 74.9, 74.8, 74.4, 73.8, 73.7, 73.4, 72.6, 69.6, 68.7, 68.5, 68.2, 67.5, 67.4, 66.6, 65.6, 63.6, 63.5, 55.2, 52.7, 52.6, 50.6, 37.5, 26.8, 26.4, 25.5, 25.4, 20.7, 20.6, 18.5, –1.4 ppm; HRMS: *m/z*: calcd for C₅₂H₆₈F₃NO₁₇Si + Na⁺: 1086.4106 [M+Na]⁺; found: 1086.4106.

2-(Trimethylsilyl)ethyl (5-amino-3,5-dideoxy-8,9-O-isopropylidene-D-glycero-α-D-galacto-2-nonulopyranosylono-1,5-lactam)-(2→6)-3,4-di-O-benzyl-2-O-p-methoxybenzyl-β-D-glucopyranoside (25): Drierite (6.3 g) was added to a solution of compound 24 (2.09 g, 2.13 mmol) in MeOH (222 mL) and the suspension was stirred for 1 h at room temperature. A 28% solution of sodium methoxide in MeOH (1.27 mL, 5.33 mmol) was added and the resulting mixture was stirred for 92 h under reflux. Completion of the reaction was confirmed by TLC (CHCl₃/MeOH 10:1), whereupon the reaction mixture was neutralized with Dowex-50 (H⁺) and filtered through Celite. The combined filtrate and washings were concentrated. The residue was subjected to column chromatography on silica gel (CHCl₃/MeOH 60:1→40:1) to give 25 (1.82 g, 95%). [α]_D = –23.0° (*c* = 1.0, CHCl₃); ¹H NMR (500 MHz, CDCl₃): δ = 7.33–6.81 (m, 14H; 3 Ar), 4.91–4.64 (m, 7H; H-5b, ArCH₂), 4.40 (d, 1H, $J_{1,2}$ =7.8 Hz; H-1a), 4.32 (brs, 1H; H-8b), 4.28 (app d, 1H; H-9b), 4.10 (m, 1H; H-4b), 4.00 (m, 4H; H-6a, H-6b, H-9'b, TMSCH₂CH₂), 3.79 (s, 3H; OMe), 3.60 (m, 6H; H-3a, H-4a, H-5a, H-6'a, H-7b, TMSCH₂CH₂), 3.37 (app t, 1H; H-2a), 2.43 (app t, 1H, J_{gem} =14.2 Hz; H-3b_{ax}), 1.97 (dd, 1H, $J_{3eq,4}$ =4.8 Hz; H-3b_{eq}), 1.36 (2 s, 6H; 2 Me), 1.05 ppm (t, 2H; TMSCH₂CH₂); ¹³C NMR (100 MHz, CDCl₃): δ = 170.4, 159.2, 138.5, 138.2, 130.5, 129.7, 128.3, 128.3, 127.9, 127.8, 127.6, 127.5, 113.7, 109.6, 103.2, 95.9, 84.6, 82.0, 77.6, 75.6, 75.3, 74.7, 74.5, 74.4, 71.0, 68.1, 67.3, 67.1, 63.4, 55.2, 54.0, 39.1, 29.6, 26.8, 25.2, 18.5, –1.5 ppm; HRMS: *m/z*: calcd for C₄₅H₆₁NO₁₃Si + Na⁺: 874.3810 [M+Na]⁺; found: 874.3811.

2-(Trimethylsilyl)ethyl [methyl 4,7,8,9-tetra-O-acetyl-3,5-dideoxy-5-(2,2,2-trichloroethoxycarbonyl)-D-glycero-α-D-galacto-2-nonulopyranosylonate]-(2→4)-(5-amino-3,5-dideoxy-8,9-O-isopropylidene-D-glycero-α-D-galacto-2-nonulopyranosylono-1,5-lactam)-(2→6)-3,4-di-O-benzyl-2-O-p-methoxybenzyl-β-D-glucopyranoside (26) and β-isomer (27): 3 Å molecular sieves (4.6 g) were added to a solution of compounds 5 (2.69 g, 3.74 mmol) and 25 (1.60 g, 1.87 mmol) in EtCN (34 mL)/CH₂Cl₂ (3.8 mL). The suspension was stirred for 1 h at room temperature, then

cooled to –40°C, whereupon NIS (1.33 g, 5.61 mmol) and TIOH (33 μL, 374 μmol) were added. Stirring was continued for 16 h, when completion of the reaction was indicated by TLC (PhMe/EtOAc 2:3). The reaction mixture was made alkaline to pH 8 with saturated aqueous NaHCO₃ solution at 0°C, filtered through Celite, and the removed molecular sieves were washed with EtOAc. The combined filtrate and washings were extracted with EtOAc, and the organic layer was washed with saturated aqueous Na₂S₂O₃ solution and brine, dried over Na₂SO₄, and concentrated. The residue was purified by column chromatography on silica gel (PhMe/EtOAc 2:1→4:3) to give 26 (1.65 g, 60%) and 27 (235 mg, 9%). 26: [α]_D = –3.0° (*c* = 1.6, CHCl₃); ¹H NMR (500 MHz, CDCl₃): δ = 7.37–6.81 (m, 14H; 3 Ar), 6.89 (d, 1H, $J_{NH,5}$ =5.9 Hz; NH-b), 5.43 (m, 1H; H-8c), 5.28 (dd, 1H, $J_{6,7}$ =2.0, $J_{7,8}$ =9.8 Hz; H-7c), 4.97–4.50 (m, 10H; H-4c, NH-c, Cl₃CCH₂, ArCH₂), 4.39 (m, 2H; H-1a, H-6b), 4.32 (dd, 1H, $J_{5,6}$ =10.7, $J_{6,7}$ =2.0 Hz; H-6c), 4.26 (dd, 1H, J_{gem} =12.2, $J_{8,9}$ =2.4 Hz; H-9c), 4.15 (m, 2H; H-6a, H-9b), 4.03 (m, 4H; H-6'a, H-5b, H-9'b, TMSCH₂CH₂), 3.89 (m, 3H; H-4b, H-8b, H-9'c), 3.76 (m, 8H; H-7b, H-5c, COOMe, OMe), 3.58 (m, 4H; H-3a, H-4a, H-5a, TMSCH₂CH₂), 3.40 (app t, 1H, $J_{1,2}$ =8.1, $J_{2,3}$ =8.6 Hz; H-2a), 2.61 (dd, 1H, J_{gem} =12.8, $J_{3eq,4}$ =4.8 Hz; H-3c_{eq}), 2.30 (dd, 1H, J_{gem} =10.6, $J_{3ax,4}$ =3.4 Hz; H-3b_{ax}), 2.19–2.01 (m, 13H; H-3b_{eq}, 4 Ac), 1.95 (app t, 1H; H-3c_{ax}), 1.43–1.38 (2 s, 6H; 2 Me), 1.06 ppm (m, 2H; TMSCH₂CH₂); ¹³C NMR (100 MHz, CDCl₃): δ = 171.6, 170.4, 170.3, 170.2, 169.2, 168.1, 159.1, 154.1, 138.7, 138.5, 130.8, 129.8, 128.3, 128.2, 127.9, 127.8, 127.5, 127.4, 113.7, 108.9, 103.1, 99.5, 95.6, 95.2, 84.7, 81.9, 78.1, 77.8, 75.6, 75.0, 74.6, 74.5, 74.3, 74.1, 72.7, 72.2, 70.9, 67.9, 67.4, 67.3, 66.8, 65.2, 63.5, 63.2, 55.2, 53.2, 52.8, 51.2, 38.0, 37.7, 29.6, 26.6, 25.7, 20.9, 20.8, 20.7, 20.6, 18.5, –1.5 ppm; HRMS: *m/z*: calcd for C₆₆H₈₇Cl₃N₂O₂₆Si + Na⁺: 1479.4280 [M+Na]⁺; found: 1479.4258. 27: [α]_D = –12.5° (*c* = 0.9, CHCl₃); ¹H NMR (600 MHz, CDCl₃): δ = 7.32–6.82 (m, 14H; 3 Ar), 6.83 (brs, 1H; NH-b), 5.42 (m, 1H; H-7c), 5.17 (m, 1H; H-4c), 5.10 (d, 1H, $J_{NH,5}$ =9.6 Hz; NH-c), 5.02 (m, 1H; H-8c), 4.90–4.47 (m, 9H; H-9c, Cl₃CCH₂, ArCH₂), 4.43 (m, 1H; H-9b), 4.38 (d, 1H, $J_{1,2}$ =8.2 Hz; H-1a), 4.24 (m, 2H; H-4b, H-8b), 4.01 (m, 5H; H-6a, H-5b, H-9'b, H-6c, TMSCH₂CH₂), 3.89 (m, 2H; H-7b, H-9c), 3.79 (m, 8H; H-6b, H-5c, COOMe, OMe), 3.61 (m, 3H; H-3a, H-4a, TMSCH₂CH₂), 3.53 (m, 2H; H-5a, H-6'a), 3.39 (app t, 1H, $J_{2,3}$ =8.3 Hz; H-2a), 3.15 (d, 1H; 7b-OH), 2.49 (dd, 1H, J_{gem} =13.0, $J_{3eq,4}$ =4.8 Hz; H-3c_{eq}), 2.37 (app t, 1H; H-3b_{ax}), 2.20 (dd, 1H, J_{gem} =13.8, $J_{3eq,4}$ =4.8 Hz; H-3b_{eq}), 2.15–2.00 (4 s, 12H; 4 Ac), 1.91 (app t, 1H; H-3c_{ax}), 1.38–1.28 (2 s, 6H; 2 Me), 1.05 ppm (m, 2H; TMSCH₂CH₂); ¹³C NMR (100 MHz, CDCl₃): δ = 170.9, 170.6, 170.1, 169.9, 169.2, 167.4, 159.1, 154.2, 138.8, 138.6, 130.8, 129.7, 128.3, 128.2, 127.8, 127.5, 127.4, 113.7, 109.2, 103.1, 99.5, 95.5, 95.3, 84.8, 81.9, 78.3, 77.6, 77.2, 75.6, 74.6, 74.5, 74.3, 74.2, 72.8, 71.7, 70.7, 70.2, 68.6, 67.9, 67.5, 66.6, 63.3, 62.1, 55.2, 53.3, 51.7, 51.1, 38.8, 36.9, 29.7, 26.7, 25.2, 20.9, 20.8, 20.7, 20.7, 18.6, –1.4 ppm; HRMS: *m/z*: calcd for C₆₆H₈₇Cl₃N₂O₂₆Si + Na⁺: 1479.4280 [M+Na]⁺; found: 1479.4280.

2-(Trimethylsilyl)ethyl [methyl 4,7,8,9-tetra-O-acetyl-3,5-dideoxy-5-(2,2,2-trichloroethoxycarbonyl)-D-glycero-α-D-galacto-2-nonulopyranosylonate]-(2→4)-(5-amino-7,8,9-tri-O-acetyl-3,5-dideoxy-D-glycero-α-D-galacto-2-nonulopyranosylono-1,5-lactam)-(2→6)-3,4-di-O-benzyl-2-O-p-methoxybenzyl-β-D-glucopyranoside (28): 80% aqueous AcOH (3.84 mL) was added to a flask containing compound 26 (225 mg, 154 μmol). The mixture was stirred for 17 h at 45°C, as the progress of the reaction was monitored by TLC (CHCl₃/MeOH 15:1). The reaction mixture was then concentrated, the remaining volatiles were co-evaporated with toluene, and the residue was exposed to high vacuum for 9 h. The crude material was redissolved in pyridine (2.24 mL) and then acetic anhydride (873 μL) was added to the solution at 0°C. The mixture was stirred for 6 h at room temperature, when completion of the reaction was confirmed by TLC (CHCl₃/MeOH 25:1). After quenching with EtOH, the mixture was concentrated and the residual volatiles were co-evaporated with toluene. The residue was redissolved in EtOAc, and this solution was washed with 2M aqueous HCl, water, saturated aqueous NaHCO₃ solution, and brine, dried (Na₂SO₄), and concentrated. The residue was purified by column chromatography on silica gel (hexane/EtOAc 4:3) to give 28 (196 mg, 82%). [α]_D = –2.5° (*c* = 1.7, CHCl₃); ¹H NMR (500 MHz, CDCl₃): δ = 7.31–6.81 (m, 14H; 3 Ar), 6.93 (d, 1H, $J_{NH,5}$ =5.9 Hz; NH-b), 5.84 (dd, 1H, $J_{6,7}$ =2.4, $J_{7,8}$ =9.4 Hz; H-7b), 5.46 (m, 2H; H-8b, H-8c), 5.27 (d, 1H, $J_{7,8}$ =9.8 Hz; H-7c), 4.99 (m, 1H; H-4c), 4.90–4.53 (m, 9H; NH-c,

Cl_3CCH_2 , ArCH_2), 4.32 (m, 6H; H-1a, H-6a, H-6b, H-9b, H-6c, H-9c), 4.15 (dd, 1H, $J_{\text{gem}}=11.4$, $J_{8,9}=5.3$ Hz; H-9'c), 3.91 (m, 12H; H-6'a, H-4b, H-5b, H-9'b, H-5c, COOMe, OMe, $\text{TMSCH}_2\text{CH}_2$), 3.56 (m, 4H; H-3a, H-4a, H-5a, $\text{TMSCH}_2\text{CH}_2$), 3.39 (app t, 1H, $J_{1,2}=7.8$, $J_{2,3}=9.0$ Hz; H-2a), 2.50 (dd, 1H, $J_{\text{gem}}=12.7$, $J_{3,4}=4.6$ Hz; H-3c_{eq}), 2.24–1.89 (m, 24H; H-3b_{ax}, H-3b_{eq}, H-3c_{ax}, 7 Ac), 1.05 ppm (app t, 2H; $\text{TMSCH}_2\text{CH}_2$); ^{13}C NMR (100 MHz, CDCl_3): $\delta=171.5$, 170.6, 170.5, 170.3, 169.9, 169.8, 169.2, 169.1, 168.7, 159.1, 157.6, 153.8, 139.5, 138.7, 138.6, 132.9, 130.8, 129.8, 129.6, 128.3, 128.2, 127.8, 127.7, 127.4, 113.7, 110.5, 103.0, 102.8, 100.3, 95.7, 95.3, 85.7, 84.6, 82.0, 81.9, 78.2, 76.2, 75.5, 74.4, 74.3, 74.0, 73.4, 72.8, 72.6, 71.9, 68.8, 67.7, 67.5, 67.3, 66.9, 63.6, 63.4, 60.9, 56.3, 55.2, 53.1, 51.6, 50.5, 37.1, 36.3, 20.9, 20.8, 20.7, 20.5, 20.5, 18.5, -1.4 ppm; HRMS: m/z : calcd for $\text{C}_{69}\text{H}_{99}\text{Cl}_3\text{N}_2\text{O}_{29}\text{Si}+\text{Na}^+$: 1565.4284 $[M+\text{Na}]^+$; found: 1565.4272.

2-(Trimethylsilyl)ethyl [methyl 4,7,8,9-tetra-O-acetyl-3,5-dideoxy-5-(2,2,2-trichloroethoxy)carbonyl-D-glycero- α -D-galacto-2-nonulopyranosylonate]-(2 \rightarrow 4)-(7,8,9-tri-O-acetyl-5-benzoyloxy)carbonyl-3,5-dideoxy-D-glycero- α -D-galacto-2-nonulopyranosylono-1,5-lactam)-(2 \rightarrow 6)-3,4-di-O-benzyl-2-O-p-methoxybenzyl- β -D-glucopyranoside (29): *N*-Benzoyloxycarbonyl succinimide (146 mg, 574 μmol) and 4-dimethylaminopyridine (DMAP) (7.0 mg, 57.4 μmol) were added to a solution of compound **28** (222 mg, 143 μmol) in pyridine (3.0 mL). The mixture was stirred for 48 h at room temperature with monitoring of the reaction by TLC (hexane/EtOAc 2:3). After quenching with EtOH, the mixture was concentrated and the residual volatiles were co-evaporated with toluene. The residue was redissolved in EtOAc, and this solution washed with 2M aqueous HCl, water, saturated aqueous NaHCO_3 solution, and brine, dried (Na_2SO_4), and concentrated. The residue was purified by column chromatography, first on silica gel (hexane/EtOAc 2:1) and then on Sephadex LH-20 ($\text{CHCl}_3/\text{MeOH}$ 1:1) to give **29** (191 mg, 79%). $[\alpha]_{\text{D}}=-0.6^\circ$ ($c=1.1$, CHCl_3); ^1H NMR (500 MHz, CDCl_3): $\delta=7.45$ –6.81 (m, 19H; 4 Ar), 5.92 (dd, 1H, $J_{6,7}=2.3$, $J_{7,8}=9.7$ Hz; H-7b), 5.55 (m, 1H; H-8c), 5.38 (d, 1H, $J_{7,8}=9.7$ Hz; H-7c), 5.30 (m, 4H; H-8b, H-4c, ArCH_2), 5.14 (d, 1H, $J_{\text{NH},5}=8.6$ Hz; NH-c), 5.00 (s, 1H; H-5b), 4.96–4.48 (m, 9H; H-6c, Cl_3CCH_2 , PhCH_2), 4.38 (d, 1H, $J_{1,2}=8.0$ Hz; H-1a), 4.35 (dd, 1H, $J_{\text{gem}}=12.6$, $J_{8,9}=2.9$ Hz; H-9c), 4.25 (m, 3H; H-4b, H-6b, H-9b), 4.12 (m, 2H; H-6a, H-9b), 4.02 (m, 2H; H-9'c, $\text{TMSCH}_2\text{CH}_2$), 3.80 (m, 7H; H-6'a, COOMe, OMe), 3.57 (m, 5H; H-3a, H-4a, H-5a, H-5c, $\text{TMSCH}_2\text{CH}_2$), 3.39 (app t, 1H, $J_{2,3}=9.2$ Hz; H-2a), 2.59 (dd, 1H, $J_{\text{gem}}=12.6$, $J_{3,4}=4.9$ Hz; H-3c_{eq}), 2.25 (m, 2H; H-3b_{ax}, H-3b_{eq}), 2.11–1.91 (m, 21H; 7 Ac), 1.55 (app t, 1H, $J_{3,4}=12.6$ Hz; H-3c_{ax}), 1.06 ppm (app t, 2H; $\text{TMSCH}_2\text{CH}_2$); ^{13}C NMR (100 MHz, CDCl_3): $\delta=170.8$, 170.7, 170.2, 169.9, 169.7, 169.5, 168.3, 164.2, 159.2, 153.6, 151.8, 138.7, 138.6, 135.1, 130.8, 129.8, 128.5, 128.3, 128.2, 128.2, 127.8, 127.8, 127.6, 127.5, 127.4, 113.7, 103.0, 98.9, 95.9, 95.6, 84.6, 81.8, 78.1, 77.2, 75.6, 75.4, 74.5, 74.3, 74.2, 73.8, 71.7, 71.2, 69.5, 69.3, 69.2, 67.4, 67.0, 63.5, 62.1, 60.7, 55.2, 53.2, 53.1, 51.0, 37.5, 35.8, 29.7, 21.0, 20.8, 20.8, 20.7, 20.5, 20.3, 18.5, -1.4 ppm; HRMS: m/z : calcd for $\text{C}_{77}\text{H}_{93}\text{Cl}_3\text{N}_2\text{O}_{31}\text{Si}+\text{Na}^+$: 1699.4651 $[M+\text{Na}]^+$; found: 1699.4626.

2-(Trimethylsilyl)ethyl [methyl 4,7,8,9-tetra-O-acetyl-3,5-dideoxy-5-(2,2,2-trichloroethoxy)carbonyl-D-glycero- α -D-galacto-2-nonulopyranosylonate]-(2 \rightarrow 4)-(7,8,9-tri-O-acetyl-5-benzoyloxy)carbonyl-3,5-dideoxy-D-glycero- α -D-galacto-2-nonulopyranosylono-1,5-lactam)-(2 \rightarrow 6)-2-O-benzoyl-3,4-di-O-benzyl- β -D-glucopyranoside (30): 2,3-Dichloro-5,6-dicyano-*p*-benzoquinone (4.4 mg, 19.4 μmol) was added to a solution of compound **29** (25.6 mg, 15.2 μmol) in CH_2Cl_2 (400 μL)/ H_2O (20 μL). The suspension was stirred for 2 h at room temperature, whereupon completion of the reaction was confirmed by TLC ($\text{CHCl}_3/\text{MeOH}$ 15:1). The mixture was diluted with CHCl_3 , and the organic layer was washed with saturated aqueous NaHCO_3 solution and brine, dried over Na_2SO_4 , concentrated, and exposed to high vacuum for 7 h. The crude material was redissolved in pyridine (500 μL) and then benzoic anhydride (16.8 mg, 74.2 μmol) and DMAP (3.0 mg, 24.6 μmol) were added to the solution. The resulting mixture was stirred for 20 h at room temperature. After completion of the reaction was indicated by TLC (PhMe/EtOAc 1:1), the reaction mixture was concentrated and the residual volatiles were co-evaporated with toluene. The residue was redissolved in EtOAc, and this solution was washed with 2M aqueous HCl, water, saturated aqueous NaHCO_3 solution, and brine, dried over Na_2SO_4 , and concentrated. The residue was

purified by column chromatography on silica gel (hexane/EtOAc 3:2 \rightarrow 1:2) to give **30** (23.7 mg, 93%). $[\alpha]_{\text{D}}=-5.7^\circ$ ($c=3.0$, CHCl_3); ^1H NMR (600 MHz, CDCl_3): $\delta=8.17$ –7.24 (m, 20H; 4 Ph), 6.09 (dd, 1H, $J_{6,7}=2.5$, $J_{7,8}=9.3$ Hz; H-7b), 5.71 (m, 1H; H-8c), 5.54 (d, 1H, $J_{7,8}=10.3$ Hz; H-7c), 5.46 (m, 4H; H-8b, H-4c, PhCH_2), 5.39 (app t, 1H, $J_{1,2}=8.2$, $J_{2,3}=9.0$ Hz; H-2a), 5.29 (d, 1H, $J_{\text{NH},5}=8.3$ Hz; NH-c), 5.16 (s, 1H; H-5b), 5.11–4.64 (m, 8H; H-1a, H-6b, Cl_3CCH_2 , PhCH_2), 4.51 (dd, 1H, $J_{\text{gem}}=12.4$, $J_{8,9}=2.8$ Hz; H-9c), 4.42 (m, 3H; H-4b, H-6b, H-9b), 4.35 (d, 1H, $J_{\text{gem}}=10.3$ Hz; H-6a), 4.27 (dd, 1H, $J_{\text{gem}}=11.4$, $J_{8,9}=4.5$ Hz; H-9'b), 4.19 (d, 1H; H-9'c), 4.14 (m, 1H; $\text{TMSCH}_2\text{CH}_2$), 3.97 (m, 5H; H-3a, H-6'a, COOMe), 3.84 (m, 2H; H-4a, H-5a), 3.68 (m, 2H; H-5c, $\text{TMSCH}_2\text{CH}_2$), 2.75 (dd, 1H, $J_{\text{gem}}=13.0$, $J_{3,4}=4.8$ Hz; H-3c_{eq}), 2.44 (m, 2H; H-3b_{ax}, H-3b_{eq}), 2.27–1.89 (7s, 21H; 7 Ac), 1.71 (app t, 1H, $J_{3,4}=13.0$ Hz; H-3c_{ax}), 1.00 ppm (app t, 2H; $\text{TMSCH}_2\text{CH}_2$); ^{13}C NMR (150 MHz, CDCl_3): $\delta=170.8$, 170.7, 170.2, 169.9, 169.7, 169.5, 168.3, 165.1, 164.3, 153.6, 151.8, 138.3, 137.8, 135.1, 132.9, 130.2, 129.7, 128.5, 128.3, 128.2, 128.1, 128.0, 127.8, 127.7, 127.5, 100.3, 98.9, 96.0, 95.6, 82.8, 78.3, 75.4, 74.9, 74.5, 74.2, 73.8, 71.6, 71.2, 69.4, 69.3, 69.2, 67.1, 67.0, 66.9, 63.5, 62.1, 60.7, 53.3, 53.1, 51.0, 37.5, 35.9, 29.6, 20.9, 20.8, 20.8, 20.6, 20.5, 20.4, 17.8, -1.5 ppm; HRMS: m/z : calcd for $\text{C}_{76}\text{H}_{91}\text{Cl}_3\text{N}_2\text{O}_{31}\text{Si}+\text{Na}^+$: 1683.4338 $[M+\text{Na}]^+$; found: 1683.4338.

2-(Trimethylsilyl)ethyl (methyl 4,7,8,9-tetra-O-acetyl-5-benzoyloxyacetamido-3,5-dideoxy-D-glycero- α -D-galacto-2-nonulopyranosylonate)-(2 \rightarrow 4)-(7,8,9-tri-O-acetyl-5-benzoyloxy)carbonyl-3,5-dideoxy-D-glycero- α -D-galacto-2-nonulopyranosylono-1,5-lactam)-(2 \rightarrow 6)-2-O-benzoyl-3,4-di-O-benzyl- β -D-glucopyranoside (31): Zinc-copper couple (7.44 g) was added to a solution of compound **30** (496 mg, 298 μmol) in acetic acid (14.9 mL) and the suspension was stirred for 45 min at room temperature. Completion of the reaction was confirmed by TLC ($\text{CHCl}_3/\text{MeOH}$ 20:1). The suspension was then filtered through Celite and the filtrate was extracted with CH_2Cl_2 . The organic layer was washed with saturated aqueous NaHCO_3 solution and brine, dried (Na_2SO_4), and concentrated. The residue was exposed to high vacuum for 30 min, and was then treated with a solution of benzoyloxyacetyl chloride (64 μL , 388 μmol) in THF (7.5 mL) for 1.5 h. The progress of the reaction was monitored by TLC ($\text{CHCl}_3/\text{MeOH}$ 20:1). Upon its completion, the mixture was diluted with EtOAc, and the organic layer was washed with saturated aqueous NaHCO_3 solution and brine, dried (Na_2SO_4), and concentrated. The residue was purified by column chromatography on silica gel (hexane/EtOAc 2:3) to give **31** (435 mg, 89%). $[\alpha]_{\text{D}}=-10.3^\circ$ ($c=1.1$, CHCl_3); ^1H NMR (500 MHz, CDCl_3): $\delta=8.16$ –7.23 (m, 25H; 5 Ph), 6.57 (d, 1H, $J_{\text{NH},5}=9.7$ Hz; NH-c), 6.03 (dd, 1H, $J_{6,7}=4.3$, $J_{7,8}=8.9$ Hz; H-7b), 5.67 (m, 1H; H-8c), 5.49 (dd, 1H, $J_{6,7}=1.7$, $J_{7,8}=10.3$ Hz; H-7c), 5.44 (m, 3H; H-8b, PhCH_2), 5.38 (app t, 1H, $J_{1,2}=8.0$, $J_{2,3}=9.2$ Hz; H-2a), 5.21 (m, 1H; H-4c), 5.11 (app t, 1H; H-5b), 4.97–4.72 (m, 6H; PhCH_2), 4.68 (d, 1H; H-1a), 4.50 (brt, 1H; H-4b), 4.40 (m, 4H; H-6b, H-9b, H-6c, H-9c), 4.29 (dd, 1H, $J_{\text{gem}}=12.0$, $J_{8,9}=5.2$ Hz; H-9c), 4.17 (m, 3H; H-9'b, H-5c, H-9'c), 4.05 (m, 2H; BnOCH_2CO), 3.96 (m, 6H; H-3a, H-6'a, COOMe, $\text{TMSCH}_2\text{CH}_2$), 3.82 (m, 2H; H-4a, H-5a), 3.66 (m, 1H; $\text{TMSCH}_2\text{CH}_2$), 2.73 (dd, 1H, $J_{\text{gem}}=12.6$, $J_{3,4}=4.6$ Hz; H-3c_{eq}), 2.39 (m, 2H; H-3b_{ax}, H-3b_{eq}), 2.26–2.07 (7s, 21H; 7 Ac), 1.94 (app t, 1H, $J_{\text{gem}}=12.6$ Hz; H-3c_{ax}), 1.00 ppm (app t, 2H; $\text{TMSCH}_2\text{CH}_2$); ^{13}C NMR (125 MHz, CDCl_3): $\delta=170.7$, 170.3, 170.1, 170.1, 169.6, 169.5, 168.2, 165.1, 164.3, 151.7, 138.2, 137.7, 136.7, 135.0, 132.8, 130.1, 129.7, 128.5, 128.4, 128.2, 128.2, 128.1, 128.0, 127.9, 127.7, 127.6, 127.5, 127.4, 100.3, 98.8, 96.0, 82.7, 78.2, 77.2, 75.6, 74.9, 74.5, 74.2, 73.7, 73.5, 73.2, 72.0, 70.6, 69.6, 69.2, 69.2, 68.8, 68.1, 67.0, 67.0, 66.6, 63.4, 62.1, 61.0, 53.5, 53.0, 48.6, 37.3, 35.8, 29.6, 22.6, 21.0, 20.8, 20.7, 20.7, 20.6, 20.5, 20.4, 17.7, -1.6 ppm; HRMS: m/z : calcd for $\text{C}_{82}\text{H}_{98}\text{N}_2\text{O}_{31}\text{Si}+\text{Na}^+$: 1657.5821 $[M+\text{Na}]^+$; found: 1657.5821.

2-(Trimethylsilyl)ethyl (methyl 4,7,8,9-tetra-O-acetyl-5-benzoyloxyacetamido-3,5-dideoxy-D-glycero- α -D-galacto-2-nonulopyranosylonate)-(2 \rightarrow 4)-(methyl 7,8,9-tri-O-acetyl-5-benzoyloxy)carbonyl-3,5-dideoxy-D-glycero- α -D-galacto-2-nonulopyranosylonate)-(2 \rightarrow 6)-2-O-benzoyl-3,4-di-O-benzyl- β -D-glucopyranoside (32): A 10% triethylamine solution in MeCN (6.0 mL) and water (3.0 mL) were added to a flask containing compound **31** (435 mg, 266 μmol). The mixture was stirred for 19 h at 40 $^\circ\text{C}$, with monitoring of the reaction by TLC ($\text{CHCl}_3/\text{MeOH}$ 10:1). Upon its completion, the mixture was concentrated and the residual volatiles were co-evaporated with toluene. The residue was redissolved in

CHCl₃, and this solution was washed with 2M aqueous HCl and brine, dried (Na₂SO₄), and concentrated, and the residue was exposed to high vacuum for 2 h. The crude material was redissolved in pyridine (2.0 mL), and acetic anhydride (500 μL) and DMAP (5.0 mg) were added to the solution. The resulting mixture was stirred for 1 h at room temperature, as the progress of the reaction was monitored by TLC (CHCl₃/MeOH 10:1). After quenching with EtOH, the mixture was concentrated and the residual volatiles were co-evaporated with toluene. The residue was redissolved in CHCl₃, and this solution was washed with 2M aqueous HCl, water, and brine, dried (Na₂SO₄), and concentrated. The residue was exposed to high vacuum for 2 h, redissolved in DMF (6.7 mL), and then iodomethane (133 μL, 2.13 mmol) and K₂CO₃ (441 mg, 3.19 mmol) were added at 0°C. The resulting mixture was stirred for 1 h at room temperature. After completion of the reaction had been indicated by TLC (CHCl₃/MeOH 20:1), triethylamine was added to the reaction mixture. The resulting mixture was extracted with EtOAc, and the combined extracts were washed with water and brine, dried (Na₂SO₄), and concentrated. The residue was purified by column chromatography on silica gel (PhMe/EtOAc 1:1) to give **32** (326 mg, 73%). [α]_D = +2.4° (c = 2.7, CHCl₃); ¹H NMR (600 MHz, CDCl₃): δ = 8.00–7.09 (m, 25H; 5 Ph), 6.25 (d, 1H, J_{NH,5} = 11.0 Hz; NH-c), 5.56 (d, 1H, J_{NH,5} = 9.7 Hz; NH-b), 5.48 (m, 3H; H-7b, H-8b, H-8c), 5.27 (m, 2H; H-7c, PhCH₂), 5.20 (app t, 1H, J_{1,2} = 8.3, J_{2,3} = 8.9 Hz; H-2a), 4.98 (d, 1H; PhCH₂), 4.87–4.52 (m, 7H; H-4c, PhCH₂), 4.44 (d, 1H; H-1a), 4.24 (dd, 1H, J_{gem} = 12.4, J_{8,9} = 2.1 Hz; H-9b), 4.20 (m, 2H; H-6a, H-9c), 4.11 (m, 1H; H-5c), 4.02 (m, 2H; H-6b, H-9'b), 3.81 (m, 15H; H-3a, H-4a, H-4b, H-5b, H-6c, H-9'c, COOMe, BnOCH₂CO, TMSCH₂CH₂), 3.60 (d, 1H, J_{gem} = 10.3 Hz; H-6'a), 3.47 (m, 2H; H-5a, TMSCH₂CH₂), 2.66 (dd, 1H, J_{gem} = 12.7, J_{3eq,4} = 4.5 Hz; H-3c_{eq}), 2.33 (m, 4H; H-3b_{eq}, Ac), 2.16–1.77 (m, 20H; H-3b_{ax}, H-3c_{ax}, 6 Ac), 0.82 ppm (m, 2H; TMSCH₂CH₂); ¹³C NMR (100 MHz, CDCl₃): δ = 170.9, 170.7, 170.5, 170.3, 170.2, 170.1, 170.0, 169.9, 167.5, 167.3, 165.2, 156.5, 138.3, 137.9, 137.8, 137.0, 136.8, 132.9, 130.1, 129.7, 129.0, 128.6, 128.4, 182.2, 128.2, 128.2, 128.0, 128.0, 127.8, 127.7, 127.5, 127.0, 100.5, 98.6, 98.3, 82.5, 77.7, 77.2, 75.0, 74.9, 74.0, 73.7, 73.5, 72.7, 72.3, 71.2, 69.2, 68.7, 68.1, 67.7, 67.4, 67.0, 66.8, 66.5, 62.9, 62.6, 62.4, 53.2, 52.1, 51.4, 48.3, 39.6, 38.2, 29.7, 21.4, 21.3, 21.2, 20.8, 20.8, 20.6, 20.4, 17.9, –1.5 ppm; HRMS: *m/z*: calcd for C₈₃H₁₀₂N₂O₃₂Si + Na⁺: 1689.6083 [M+Na]⁺; found: 1689.6083.

2-(Trimethylsilyl)ethyl (methyl 4,7,8,9-tetra-O-acetyl-5-acetoxyacetamido-3,5-dideoxy-D-glycero-α-D-galacto-2-nonulopyranosylonate)-(2→4)-(methyl 5-acetamido-7,8,9-tri-O-acetyl-3,5-dideoxy-D-glycero-α-D-galacto-2-nonulopyranosylonate)-(2→6)-3,4-di-O-acetyl-2-O-benzoyl-β-D-glucopyranoside (33): 20% Pd(OH)₂ on activated carbon (273 mg) was added to a solution of compound **32** (273 mg, 164 μmol) in EtOH (6.2 mL)/THF (2.0 mL)/AcOH (0.8 mL) and the suspension was stirred under a hydrogen stream for 1 h at room temperature. After completion of the reaction had been indicated by TLC (CHCl₃/MeOH 10:1), the reaction mixture was filtered through Celite and the filtrate was concentrated. The residue was exposed to high vacuum for 12 h. The crude material was redissolved in pyridine (2.0 mL), and acetic anhydride (1.0 mL) and DMAP (5.0 mg) were added to the solution. The resulting mixture was stirred for 6.5 h at room temperature with monitoring of the reaction by TLC (CHCl₃/MeOH 15:1). After quenching with EtOH, the mixture was concentrated and the remaining volatiles were co-evaporated with toluene. The residue was redissolved in EtOAc, and this solution was washed with 2M aqueous HCl, water, saturated aqueous NaHCO₃ solution, and brine, dried (Na₂SO₄), and concentrated. The residue was purified by column chromatography on silica gel (CHCl₃/MeOH 50:1) to give **33** (209 mg, 89%). [α]_D = +4.3° (c = 2.0, CHCl₃); ¹H NMR (600 MHz, CDCl₃): δ = 8.00–7.42 (m, 5H; Ph), 6.05 (d, 1H, J_{NH,5} = 10.3 Hz; NH-b), 5.78 (d, 1H, J_{NH,5} = 9.6 Hz; NH-c), 5.60 (m, 1H; H-8c), 5.45 (dd, 1H, J_{6,7} = 2.1, J_{7,8} = 8.3 Hz; H-7b), 5.41 (m, 1H; H-8b), 5.35 (t, 1H, J_{2,3} = J_{3,4} = 9.6 Hz; H-3a), 5.23 (m, 2H; H-2a, H-4a), 5.16 (dd, 1H, J_{6,7} = 2.1, J_{7,8} = 8.9 Hz; H-7c), 4.81 (m, 1H; H-4c), 4.57 (d, 1H, J_{gem} = 15.8 Hz; AcOCH₂CO), 4.56 (d, 1H, J_{1,2} = 8.2 Hz; H-1a), 4.40 (dd, 1H, J_{gem} = 11.7, J_{8,9} = 1.3 Hz; H-9c), 4.35 (dd, 1H, J_{gem} = 12.0, J_{8,9} = 2.4 Hz; H-9b), 4.27 (d, 1H; AcOCH₂CO), 4.05 (m, 3H; H-5b, H-9'b, H-5c), 3.89 (m, 11H; H-6a, H-6b, H-6c, H-9'c, COOMe, TMSCH₂CH₂), 3.65 (m, 2H; H-5a, H-4b), 3.52 (m, 2H; H-6'a, TMSCH₂CH₂), 2.62 (dd, 1H, J_{gem} = 12.8, J_{3eq,4} =

4.5 Hz; H-3c_{eq}), 2.22 (dd, 1H, J_{gem} = 12.8, J_{3eq,4} = 3.7 Hz; H-3b_{eq}), 2.18–1.88 (m, 34H; H-3c_{ax}, 11 Ac), 1.79 (app t, 1H; H-3b_{ax}), 0.81 ppm (m, 2H; TMSCH₂CH₂); ¹³C NMR (100 MHz, CDCl₃): δ = 171.9, 171.2, 170.6, 170.5, 170.4, 170.4, 170.1, 170.0, 169.6, 169.1, 167.7, 167.6, 167.1, 165.0, 133.2, 129.8, 129.5, 128.4, 100.5, 98.5, 98.0, 77.6, 77.2, 73.2, 72.5, 72.4, 72.2, 71.8, 71.3, 68.4, 68.0, 67.7, 67.6, 67.5, 67.2, 64.0, 62.7, 53.1, 52.3, 49.1, 48.8, 38.7, 38.2, 29.7, 23.3, 21.2, 21.2, 20.9, 20.9, 20.8, 20.7, 20.7, 20.7, 20.6, 20.6, 17.8, –1.5 ppm; HRMS: *m/z*: calcd for C₆₂H₈₆N₂O₃₄Si + Na⁺: 1453.4729 [M+Na]⁺; found: 1453.4728.

(Methyl 4,7,8,9-tetra-O-acetyl-5-acetoxyacetamido-3,5-dideoxy-D-glycero-α-D-galacto-2-nonulopyranosylonate)-(2→4)-(methyl 5-acetamido-7,8,9-tri-O-acetyl-3,5-dideoxy-D-glycero-α-D-galacto-2-nonulopyranosylonate)-(2→6)-3,4-di-O-acetyl-2-O-benzoyl-α-D-glucopyranosyl trichloroacetimidate (34): CF₃COOH (500 μL) was added to a solution of compound **33** (70.0 mg, 48.9 μmol) in CH₂Cl₂ (1.0 mL) at 0°C. The mixture was stirred for 4 h at room temperature with monitoring of the reaction by TLC (CHCl₃/MeOH 10:1), then concentrated, and the remaining volatiles were co-evaporated with toluene. The residue was subjected to column chromatography on silica gel (CHCl₃/MeOH 35:1) to give the 1-OH derivative (63.8 mg). This compound was exposed to high vacuum for 12 h and then redissolved in CH₂Cl₂ (1.0 mL). Trichloroacetoneitrile (49 μL, 489 μmol) and 1,8-diazabicyclo[5.4.0]undec-7-ene (2.2 μL, 14.7 μmol) were added to the solution, and the resulting mixture was stirred for 1 h at 0°C. Completion of the reaction was confirmed by TLC (CHCl₃/MeOH 10:1). The mixture was concentrated, and the residue was purified by column chromatography (CHCl₃/MeOH 40:1) to give **34** (62.5 mg, 87%). [α]_D = +41.6° (c = 0.7, CHCl₃); ¹H NMR (400 MHz, CDCl₃): δ = 8.52 (s, 1H; Cl₃CCNH), 7.98–7.40 (m, 5H; Ph), 6.67 (d, 1H, J_{1,2} = 3.7 Hz; H-1a), 6.03 (d, 1H, J_{NH,5} = 10.5 Hz; NH-b), 5.76 (d, 1H, J_{NH,5} = 10.1 Hz; NH-c), 5.75 (app t, 1H, J_{2,3} = 10.1, J_{3,4} = 9.6 Hz; H-3a), 5.61 (m, 1H; H-8b), 5.39 (m, 4H; H-2a, H-4a, H-7c, H-8c), 5.16 (dd, 1H, J_{6,7} = 2.3, J_{7,8} = 8.7 Hz; H-7b), 4.81 (m, 1H; H-4c), 4.58 (d, 1H, J_{gem} = 15.1 Hz; AcOCH₂CO), 4.40 (dd, 1H, J_{gem} = 12.2, J_{8,9} = 2.3 Hz; H-9b), 4.31 (dd, 1H, J_{5,6} = 12.4, J_{6,7} = 2.8 Hz; H-6c), 4.27 (d, 1H; AcOCH₂CO), 4.20 (brd, 1H; H-5a), 3.96 (m, 13H; H-6a, H-5b, H-6b, H-9'b, H-5c, H-6c, H-9'c, COOMe), 3.65 (m, 1H; H-4b), 3.42 (app d, 1H; H-6'a), 2.62 (dd, 1H, J_{gem} = 12.6, J_{3eq,4} = 4.4 Hz; H-3c_{eq}), 2.34–1.97 (m, 34H; H-3b_{eq}, 11 Ac), 1.90 (app t, 1H; H-3c_{ax}), 1.83 ppm (app t, 1H, J_{gem} = 12.6 Hz; H-3b_{ax}); ¹³C NMR (100 MHz, CDCl₃): δ = 171.9, 171.2, 170.6, 170.5, 170.4, 170.2, 170.0, 169.6, 168.8, 167.7, 167.6, 167.0, 165.3, 160.6, 133.6, 129.8, 128.6, 128.5, 98.3, 98.0, 93.2, 90.7, 77.2, 72.5, 72.2, 71.3, 70.8, 70.4, 70.2, 68.3, 67.9, 67.6, 67.5, 67.2, 67.1, 64.0, 62.7, 61.6, 53.0, 52.5, 49.1, 48.8, 38.7, 38.1, 31.9, 30.0, 29.7, 29.3, 23.3, 22.6, 21.2, 20.9, 20.8, 20.8, 20.7, 20.7, 20.6, 14.1 ppm; MALDI-TOF MS: *m/z*: calcd for C₅₉H₇₄Cl₃N₅O₃₄ + Na⁺: 1496.3 [M+Na]⁺; found: 1496.3.

(2S,3R,4E)-2-N-tert-Butoxycarbonyl-10,2N-isopropylidene-3-hydroxy-15-methylhexadec-4-ene (37): [Cp₂Zr(H)Cl] (2.20 g, 8.54 mmol) was added to a solution of compound **12** (1.17 g, 6.17 mmol) in THF (12.0 mL) at 0°C and the resulting mixture was stirred for 1 h at room temperature and then cooled to 0°C once more. The resulting yellow solution was treated first with a solution of **11** (1.09 g, 4.75 mmol) in THF (12 mL) and then with zinc bromide (270 mg, 1.19 mmol) and the mixture was stirred for 18 h at room temperature. Completion of the reaction was confirmed by TLC (CHCl₃/MeOH 10:1). After the addition of Rochelle salt, the suspension was filtered through Celite and the filtrate was extracted with EtOAc. The organic phase was washed with water and brine, dried over Na₂SO₄, and concentrated. The residue was purified by column chromatography on silica gel (hexane/EtOAc 10:1→8:1) to give **37** (1.06 g, 56%). [α]_D = –39.1° (c = 1.0, CHCl₃); ¹H NMR (400 MHz, CDCl₃): δ = 5.75 (m, 1H), 5.45 (dd, 1H, J = 5.1, 15.7 Hz), 4.14 (m, 2H), 4.03 (brs, 1H), 3.84 (brs, 1H), 2.05 (m, 2H), 1.54 (m, 15H; 5 Me), 1.36 (m, 2H), 1.20 (m, 15H; -CH₂-, H-15), 0.86 ppm (d, 6H, J = 6.6 Hz; CH-(CH₂)₂); ¹³C NMR (100 MHz, CDCl₃): δ = 133.4, 128.1, 94.4, 74.0, 64.9, 62.3, 39.0, 32.4, 32.3, 31.9, 29.9, 29.6, 29.5, 29.3, 29.2, 29.1, 29.0, 28.4, 27.9, 27.4, 26.2, 24.6, 22.6, 14.1 ppm; HRMS: *m/z*: calcd for C₂₅H₄₉NO₄ + Na⁺: 448.3403 [M+Na]⁺; found: 448.3405.

(2S,3R,4E)-2-N-tert-Butoxycarbonyl-15-methylhexadec-4-ene-1,3-diol (38): 80% aqueous AcOH (14.0 mL) was added to a flask containing

compound **37** (614 mg, 1.44 mmol). The mixture was stirred for 4 h at 45 °C, as the progress of the reaction was monitored by TLC (hexane/EtOAc 1:1). The reaction mixture was then concentrated, the remaining volatiles were co-evaporated with toluene, and the residue was extracted with CHCl₃. The organic phase was washed with water, saturated aqueous NaHCO₃ solution, and brine, dried over Na₂SO₄, and concentrated. The residue was purified by column chromatography on silica gel (hexane/EtOAc 3:1) to give **38** (372 mg, 67%). [α]_D = -3.6° (c = 1.8, CHCl₃); ¹H NMR (400 MHz, CDCl₃): δ = 5.77 (m, 1H), 5.52 (dd, 1H, *J* = 6.6, 15.4 Hz), 5.36 (d, 1H, *J* = 8.1 Hz; NH), 4.29 (br, 1H), 3.81 (m, 2H), 3.60 (brs, 1H), 3.11 (brs, 1H), 2.05 (m, 2H), 1.50 (m, 9H; 3 Me), 1.37 (m, 2H), 1.19 (m, 15H; -CH₂-, H-15), 0.86 ppm (d, 6H, *J* = 6.6 Hz; CH-(CH₃)₂); ¹³C NMR (100 MHz, CDCl₃): δ = 156.2, 134.0, 133.8, 128.9, 79.7, 74.6, 73.1, 64.1, 55.4, 39.0, 32.3, 29.9, 29.7, 29.6, 29.5, 29.2, 29.1, 28.5, 28.3, 28.1, 27.9, 27.7, 27.5, 27.4, 22.6 ppm; HRMS: *m/z*: calcd for C₂₂H₄₃NO₄ + Na⁺: 408.3090 [*M*+Na]⁺; found: 408.3097.

(2S,3R,4E)-2-Amino-15-methylhexadec-4-ene-1,3-diol (39): CF₃COOH (2.68 mL, 35.0 mmol) was added to a solution of compound **38** (90 mg, 233 μ mol) in CH₂Cl₂ (4.66 mL). The mixture was stirred for 15 min at room temperature, as the progress of the reaction was monitored by TLC (CHCl₃/MeOH 3:1). The reaction mixture was then concentrated, the remaining volatiles were co-evaporated with toluene, and the residue was extracted with CHCl₃. The organic phase was washed with saturated aqueous NaHCO₃ solution, dried over Na₂SO₄, and concentrated. The residue was purified by column chromatography on silica gel (CHCl₃/MeOH 10:1→3:1) to give **39** (54 mg, 81%). [α]_D = -14.7° (c = 1.8, CHCl₃); ¹H NMR (400 MHz, CDCl₃): δ = 5.76 (m, 1H), 5.47 (dd, 1H, *J* = 7.0, 15.4 Hz), 4.06 (m, 1H), 3.65 (m, 2H), 2.87 (brs, 1H), 2.54 (brs, 2H; NH₂), 2.06 (m, 2H), 1.51 (m, 1H), 1.37 (m, 2H), 1.19 (m, 14H; -CH₂-), 0.86 ppm (d, 6H, *J* = 6.6 Hz; CH(CH₃)₂); ¹³C NMR (100 MHz, CDCl₃): δ = 134.6, 134.1, 129.2, 75.1, 63.7, 56.1, 39.0, 32.3, 29.9, 29.7, 29.6, 29.5, 29.2, 27.9, 27.4, 22.6 ppm; HRMS: *m/z*: calcd for C₁₇H₃₃NO₂ + Na⁺: 308.2565 [*M*+Na]⁺; found: 308.2520.

1-Icosanal (41): NaHCO₃ (631 mg, 7.51 mmol) and Dess–Martin periodinane (251 mg, 593 μ mol) were added to a solution of compound **40** (118 mg, 395 μ mol) in CH₂Cl₂ (7.90 mL). The mixture was stirred for 1 h at room temperature with monitoring of the reaction by TLC (hexane/EtOAc 8:1). After quenching with saturated aqueous NaHCO₃ solution and saturated aqueous Na₂S₂O₃ solution, the mixture was extracted with CHCl₃. The organic phase was washed with water and brine, dried over Na₂SO₄, and concentrated. The residue was purified by column chromatography on silica gel (hexane/EtOAc 20:1) to give **41** (104 mg, 89%). The spectral data were identical to those of the known compound.^[34]

1,1-Dibromohexicos-1-ene (42): PPh₃ (6.08 g, 23.2 mmol) was added to a solution of CBr₄ (3.85 g, 11.6 mmol) in CH₂Cl₂ (48 mL). The mixture was stirred for 5 min at 0 °C, and then **41** (1.72 g, 5.80 mmol) was added. The reaction mixture was stirred for 30 min at 0 °C and was then allowed to warm to room temperature. After stirring for 1.5 h at room temperature, water was added and the resulting mixture was extracted with CHCl₃. The organic phase was washed with saturated aqueous NaHCO₃ solution and brine, dried over Na₂SO₄, and concentrated. The residue was purified by column chromatography on silica gel (hexane) to give **42** (2.52 g, 96%). [α]_D = -0.6° (c = 0.8, CHCl₃); ¹H NMR (400 MHz, CDCl₃): δ = 6.38 (t, 1H, *J* = 7.3 Hz), 2.09 (q, 2H, *J* = 7.3 Hz), 1.26 (m, 34H; -CH₂-), 0.88 ppm (t, 3H, *J* = 6.8 Hz; CH₃CH₂); ¹³C NMR (100 MHz, CDCl₃): δ = 138.9, 88.4, 33.0, 31.9, 29.7, 29.6, 29.5, 29.4, 29.3, 29.0, 27.8, 22.7, 14.1 ppm; FAB-MS: *m/z*: calcd for C₂₁H₄₀Br₂-2H: 448 [*M*-2H]⁺; found: 448.

1-Hexicosyne (15): At -78 °C, a 1.6M solution of *n*BuLi in hexane (5.98 mL, 9.57 mmol) was added to a solution of compound **42** (1.44 g, 3.19 mmol) in THF (10.6 mL). The reaction mixture was stirred for 1 h at room temperature. Completion of the reaction was confirmed by TLC (hexane). After the addition of water, the mixture was extracted with Et₂O. The organic phase was washed with water and brine, dried over Na₂SO₄, and concentrated. The residue was purified by column chromatography on silica gel (hexane) to give **15** (903 mg, 97%). The spectral data were identical to those of the known compound.^[30]

(2S,3R,4E)-2-[(R)-2-(Benzoyloxy)tetracosanoylamino]-15-methylhexadec-4-ene-1,3-diol (47): 1-Ethyl-3-(3-dimethylaminopropyl)carbodiimide hydrochloride (225 mg, 1.18 mmol) was added to a solution of compounds **39** (112 mg, 392 μ mol) and **46** (230 mg, 470 μ mol) in CH₂Cl₂ (8.0 mL) at 0 °C. After stirring for 15 min at 0 °C, the reaction mixture was gradually allowed to warm to room temperature, and stirring was continued for 18 h until TLC analysis (CHCl₃/MeOH 10:1) indicated completion of the reaction. The reaction mixture was extracted with CHCl₃ and the organic phase was washed with saturated aqueous NaHCO₃ solution, dried over Na₂SO₄, and concentrated. The residue was purified by column chromatography on silica gel (CHCl₃/MeOH, 100:1) to give **47** (203 mg, 68%). [α]_D = -17.6° (c = 0.7, CHCl₃); ¹H NMR (600 MHz, CDCl₃): δ = 8.09–7.47 (m, 5H; Ph), 6.88 (d, 1H, *J* = 7.6 Hz; NH), 5.79 (m, 1H), 5.51 (dd, 1H, *J* = 6.2, 15.8 Hz), 5.36 (t, 1H, *J* = 6.2 Hz), 4.36 (q, 1H), 3.97 (m, 1H), 3.89 (m, 1H), 3.70 (m, 1H), 2.69 (d, 1H), 2.60 (q, 1H), 2.00 (m, 4H), 1.50 (m, 3H), 1.24 (m, 54H; -CH₂-), 0.88 ppm (m, 9H; CH₂CH₂, (CH₃)₂CH); ¹³C NMR (150 MHz, CDCl₃): δ = 170.5, 165.7, 134.2, 133.6, 129.7, 129.2, 128.6, 128.5, 74.9, 73.8, 61.9, 54.5, 39.0, 32.2, 31.9, 29.9, 29.7, 29.6, 29.6, 29.5, 29.4, 29.3, 29.3, 29.2, 29.0, 27.9, 27.4, 24.9, 22.7, 22.6, 14.1 ppm; HRMS: *m/z*: calcd for C₄₈H₈₈NO₃ + Na⁺: 778.6325 [*M*+Na]⁺; found: 778.6322.

(2S,3R,4E)-2-[(R)-2-(Benzoyloxy)tetracosanoylamino]-15-methyl-1-O-triisopropylsilylhexadec-4-ene-1,3-diol (48): Imidazole (147 mg, 2.16 mmol) and TIPSCl (185 μ L, 865 μ mol) were added to a solution of compound **47** (327 mg, 432 μ mol) in DMF (2.2 mL). The mixture was stirred for 2.5 h at room temperature with monitoring of the reaction by TLC (hexane/EtOAc 3:1). After quenching with MeOH, the mixture was extracted with EtOAc. The organic phase was washed with water and brine, dried over Na₂SO₄, and concentrated. The residue was purified by column chromatography on silica gel (hexane/EtOAc 20:1) to give **48** (328 mg, 83%). [α]_D = +1.8° (c = 0.9, CHCl₃); ¹H NMR (600 MHz, CDCl₃): δ = 8.09–7.45 (m, 5H; Ph), 7.05 (d, 1H, *J* = 8.3 Hz; NH), 5.81 (m, 1H), 5.54 (m, 2H), 4.24 (brs, 1H), 4.09 (dd, 1H, *J* = 2.7, 10.3 Hz), 3.99 (m, 1H), 3.78 (dd, 1H, *J* = 2.7, 10.3 Hz), 3.41 (d, 1H), 2.00 (m, 4H), 1.52 (m, 1H), 1.31 (m, 56H; -CH₂-), 0.91 ppm (m, 30H; CH₃CH₂, (CH₃)₂CH, ((CH₃)₂CH)₃Si); ¹³C NMR (150 MHz, CDCl₃): δ = 169.8, 164.9, 133.4, 133.3, 129.7, 129.3, 129.2, 128.5, 74.3, 74.3, 63.6, 53.0, 39.0, 32.3, 32.2, 31.9, 29.9, 29.7, 29.6, 29.6, 29.5, 29.5, 29.4, 29.3, 29.3, 29.1, 27.9, 27.4, 24.8, 22.7, 22.6, 17.9, 17.7, 17.3, 14.1, 11.7, 11.5, 11.3 ppm; HRMS: *m/z*: calcd for C₅₇H₁₀₅NO₃Si + Na⁺: 934.7660 [*M*+Na]⁺; found: 934.7660.

(2S,3R,4E)-3-O-Benzoyl-2-[(R)-2-(benzoyloxy)tetracosanoylamino]-15-methyl-1-O-triisopropylsilylhexadec-4-ene-1,3-diol (49): Benzoic anhydride (244 mg, 1.08 mmol) and DMAP (4.0 mg, 32.7 μ mol) were added to a solution of compound **48** (328 mg, 359 μ mol) in pyridine (3.0 mL). The mixture was stirred for 17 h at room temperature with monitoring of the reaction by TLC (hexane/EtOAc 10:1). After quenching with water, the mixture was extracted with EtOAc. The organic phase was washed with 2M aqueous HCl, water, saturated aqueous NaHCO₃ solution, and brine, dried over Na₂SO₄, and concentrated. The residue was purified by column chromatography on silica gel (hexane/EtOAc 25:1) to give **49** (361 mg, 99%). [α]_D = +19.0° (c = 1.0, CHCl₃); ¹H NMR (600 MHz, CDCl₃): δ = 8.04–7.40 (m, 10H; 2 Ph), 6.67 (d, 1H, *J* = 9.6 Hz; NH), 5.92 (m, 1H), 5.61 (m, 2H), 5.52 (m, 1H), 4.44 (m, 1H), 3.95 (dd, 1H, *J* = 2.8, 10.4 Hz), 3.70 (dd, 1H, *J* = 4.1, 10.4 Hz), 1.98 (m, 4H), 1.51 (m, 1H), 1.20 (m, 56H; -CH₂-), 0.88 ppm (m, 30H; CH₃CH₂, (CH₃)₂CH, ((CH₃)₂CH)₃Si); ¹³C NMR (125 MHz, CDCl₃): δ = 169.4, 165.2, 164.9, 137.0, 133.4, 132.8, 130.3, 129.7, 129.6, 129.3, 128.5, 128.3, 124.9, 74.4, 73.9, 61.9, 52.0, 39.0, 32.3, 32.2, 31.9, 29.9, 29.7, 29.6, 29.5, 29.4, 29.3, 29.3, 28.8, 27.9, 27.4, 24.9, 22.7, 22.6, 17.7, 17.7, 14.1, 11.7, 11.6 ppm; HRMS: *m/z*: calcd for C₆₄H₁₀₉NO₆Si + Na⁺: 1038.7922 [*M*+Na]⁺; found: 1038.7922.

(2S,3R,4E)-3-O-Benzoyl-2-[(R)-2-(benzoyloxy)tetracosanoylamino]-15-methylhexadec-4-ene-1,3-diol (50): A 1M solution of TBAF in THF (212 μ L, 212 μ mol) and AcOH (50 μ L, 850 μ mol) were added to a solution of compound **49** (108 mg, 106 μ mol) in THF (520 μ L). The mixture was stirred for 24 h at room temperature with monitoring of the reaction by TLC (hexane/EtOAc 4:1). The mixture was then diluted with EtOAc, washed with water and brine, dried over Na₂SO₄, and concentrated. The